Aspects of PET-CT in prostate cancer. Protocol optimization, diagnostic accuracy, and dosimetry.

Björsdorff, Mimmi

2022

Document Version:
Publisher's PDF, also known as Version of record

Aspects of PET-CT in prostate cancer

Protocol optimization, diagnostic accuracy, and dosimetry

MIMMI BJÖERSDORFF
CLINICAL PHYSIOLOGY AND NUCLEAR MEDICINE, MALMÖ | LUND UNIVERSITY

Aspects of PET-CT in prostate cancer: protocol optimization, diagnostic accuracy, and dosimetry

This thesis evaluates aspects of PET-CT in prostate cancer. The aim is to better help patients with intermediate- and high-risk prostate cancer to reach a more accurate and correct diagnosis and staging of the disease. This has been done by searching for the most optimal settings of the PET-CT system for the examination, assess the accuracy of detecting regional lymph node metastases, and investigate the distribution and dosimetry of the tracer used in the examination. In conclusion, the thesis showed a poor performance of the examination method [^{18}F]FCH PET-CT to predict lymph node metastases. The research work also showed that the BSREM reconstruction algorithm is advantageous over OSEM, and that the calculated effective dose of [^{18}F]PSMA-1007 is on par with other commonly used PET-radiopharmaceuticals.

MIMMI BJÖERSDORFF graduated from the University of Gothenburg in 2013 as a Biomedical laboratory scientist with a specialization in Clinical physiology (Technologist). In 2015, Mimmi graduated with a master's degree in Business Creation and Entrepreneurship in Biomedicine. After two years at the Department of Clinical Physiology at Linköping University Hospital, she moved to the Department of Clinical Physiology and Nuclear Medicine at Skåne University Hospital in Malmö. 2017, Mimmi was admitted as a PhD-student at the Department of Translational Medicine, Faculty of Medicine at Lund University.

Printed by Media-Tryck, Lund 2022 NORDIC SWAN ECOLABEL 3041 0903

LUND UNIVERSITY

FACULTY OF MEDICINE

Department of Translational Medicine
Clinical Physiology and Nuclear Medicine, Malmö

Lund University, Faculty of Medicine
Doctoral Dissertation Series 2022:19
ISBN 978-91-8021-180-2
ISSN 1652-8220

Aspects of PET-CT in prostate cancer
- protocol optimization, diagnostic accuracy, and dosimetry

Aspects of PET-CT in prostate cancer

Protocol optimization, diagnostic accuracy, and dosimetry

Mimmi Björsdorff

LUND
UNIVERSITY

DOCTORAL DISSERTATION

by due permission of the Faculty of Medicine, Lund University, Sweden.
To be defended at the Department of Clinical Physiology and Nuclear Medicine,
Carl Bertil Laurells gata 9, Skåne University Hospital, Malmö, in room 2005/2007
February 11, 2022, at 09.00 a.m.

Faculty opponent
PhD Maria Holstensson, Department of Clinical Science, Intervention and Technology, Karolinska Institutet

Organization LUND UNIVERSITY Faculty of Medicine Department of Translational Medicine Clinical Physiology and Nuclear Medicine, Malmö	**Document name** DOCTORAL DISSERTATION
	Date of issue February 11 2022
Author Mimmi Björsdorff	Sponsoring organization

Title Aspects of PET-CT in prostate cancer: protocol optimization, diagnostic accuracy, and dosimetry

Abstract

The PET-CT imaging modality is based on positron emission tomography combined with computed tomography. Before a PET-CT examination, a radioactive tracer (also called a radiopharmaceutical) is intravenously injected into the patient. PET technology images the distribution of this tracer element by detecting the decay. In recent years, PET technology has been developed and improved in hardware and software. In addition, new radioactive tracers have been introduced.

Prostate cancer is one of the most common cancers affecting men. PET-CT is used to evaluate the suspected primary tumour, for staging, to evaluate the treatment, and to diagnose suspected recurrences. In 2017, the PET-CT machine park at Skåne University Hospital was upgraded from conventional PET-CT systems to newly developed and improved PET-CT systems.

Previously, the radioactive tracer [^{18}F]fluorocholine ([^{18}F]FCH) was used in PET-CT examinations of prostate cancer at Skåne University Hospital. However, [^{18}F]FCH is not specific or sensitive enough to examine prostate cancer, and therefore, in 2019, it was replaced by [^{18}F]prostate-specific membrane antigen-1007 ([^{18}F]PSMA-1007).

In a optimization study, the protocol for the [^{18}F]FCH examination method was optimized for the new PET-CT system in terms of frame duration time and value of the noise reduction factor, β. For injection of 4 MBq/kg [^{18}F]FCH, a frame duration of 1.5 min/bed position with a β-value of 400–550 was required to obtain good image quality.

The accuracy of [^{18}F]FCH PET-CT for staging primary lymph node metastases has been validated, with low sensitivity (43%) and moderate specificity (70%) reported. To examine these results more in-depth, a second study was conducted. In this study, the conventional and novel PET-CT systems were validated based on their ability to accurately detect regional lymph node metastases. This study found large differences in sensitivity and specificity between the PET-CT systems but with almost similar total diagnostic ability. Both studies used histopathology from extended pelvic lymph node dissection as a reference method.

Through a biokinetic and dosimetric study of [^{18}F]PSMA-1007 in patients with prostate cancer, the last study aimed to calculate the absorbed doses and effective dose. The effective dose was calculated to 25 μSv/MBq, corresponding to approximately 8 mSv for a ”standard patient”.

In conclusion, this thesis shows that the reconstruction algorithm BSREM is advantageous over OSEM using [^{18}F]FCH PET-CT, but that the diagnostic accuracy of [^{18}F]FCH PET-CT in detecting pelvic lymph node metastases is not good enough. Furthermore, the thesis shows that the effective dose generated by [^{18}F]PSMA-1007 supporting continued use with the radiopharmaceutical in diagnostic imaging.

Keywords PET-CT, prostate cancer, [^{18}F]FCH, [^{18}F]PSMA-1007, optimization, diagnostic accuracy, dosimetry

Classification system and/or index terms (if any)

Supplementary bibliographical information		**Language** English
ISSN 1652-8220		**ISBN** 978-91-8021-180-2
Recipient’s notes	**Number of pages** 72	Price
	Security classification	

Signature  Date 2022-01-03

Aspects of PET-CT in prostate cancer

Protocol optimization, diagnostic accuracy, and dosimetry

Mimmi Björsdorff

Cover picture by William Bjöersdorff

Faculty of Medicine, Lund University
Department of Translational Medicine,
Clinical Physiology and Nuclear Medicine, Malmö

ISBN 978-91-8021-180-2
ISSN 1652-8220

Printed in Sweden by Media-Tryck, Lund University, Lund 2022

”Vår uppgift som forskare
är att byta åsikter mot insikter”

- Lars Roepstorff, Professor,
Sveriges Lantbruksuniversitet

Table of Contents

List of papers

The following papers are the base of this thesis, referred in the text by their Roman numerals.

I. **Mimmi Björsdorff**, Jenny Oddstig, Nina Karindotter-Borgendahl, Helén Almquist, Sophia Zackarisson, David Minarik and Elin Trägårdh: Impact of penalizing factor in a block-sequential regularization reconstruction algorithm for [^{18}F]fluorocholine PET-CT regarding image quality and interpretation. EJNMMI Physics 2019;6:5 (doi.org/10.1186/s40658-019-0242-2, 6:5 2019)

II. Christopher Puterman, **Mimmi Björsdorff**, Jennifer Amidi, Aseem Anand, Wolfgang Soller, Thomas Jiborn, Henrik Kölhede, Elin Trägårdh, Anders Bjartell: A retrospective study assessing the accuracy of [^{18}F]fluorocholine PET/CT for primary staging of lymph node metastases in intermediate and high-risk prostate cancer patients undergoing robotic-assisted laparoscopic prostatectomy with extended lymph node dissection. Scand J Urol 2021;55:293-297 (doi: 10.1080/21681805.2021.1914720)

III. **Mimmi Björsdorff**, Christopher Puterman, Jenny Oddstig, Jennifer Amidi, Sophia Zackarisson, Henrik Kjölhede, Anders Bjartell, Per Wollmer, Elin Trägårdh: Detection of lymph node metastases in patients with prostate cancer: Comparing conventional and digital [^{18}F]fluorocholine PET-CT using extended pelvic lymph node dissection as a reference – a retrospective cohort study. (Submitted)

IV. Erland Hvittfeldt, **Mimmi Björsdorff**, Sigrid Leide Svegborn, Jenny Oddstig, Gustav Brolin, David Minarik, Elin Trägårdh: Biokinetics and dosimetry of [^{18}F]PSMA-1007 in patients with prostate cancer. (Submitted)

My contributions to each paper

	Study design	Ethical application	Data collection	Data analysis	Statistical analysis	Figures and tables	Interpretation of the results	Preparation of manuscript	Revision of manuscript	Response to reviewers
Paper I	1	0	3	3	1	2	2	3	2	3
Paper II	2	0	3	3	3	3	3	3	3	2
Paper III	3	0	3	3	3	3	3	3	-	-
Paper IV	2	0	3	2	1	2	2	2	-	-

Not applicable	-
No contribution	0
Limited contribution	1
Moderate contribution	2
Significant contribution	3

Abstract

The PET-CT imaging modality is based on positron emission tomography combined with computed tomography. Before a PET-CT examination, a radioactive tracer (also called a radiopharmaceutical) is intravenously injected into the patient. PET technology images the distribution of this tracer element by detecting the decay. In recent years, PET technology has been developed and improved in hardware and software. In addition, new radioactive tracers have been introduced.

Prostate cancer is one of the most common cancers affecting men. PET-CT is used to evaluate the suspected primary tumour, for staging, to evaluate the treatment, and to diagnose suspected recurrences. In 2017, the PET-CT machine park at Skåne University Hospital was upgraded from conventional PET-CT systems to newly developed and improved PET-CT systems.

Previously, the radioactive tracer [^{18}F]fluorocholine ([^{18}F]FCH) was used in PET-CT examinations of prostate cancer at Skåne University Hospital. However, [^{18}F]FCH is not specific or sensitive enough to examine prostate cancer, and therefore, in 2019, it was replaced by [^{18}F]prostate-specific membrane antigen-1007 ([^{18}F]PSMA-1007).

In a optimization study, the protocol for the [^{18}F]FCH examination method was optimized for the new PET-CT system in terms of frame duration time and value of the noise reduction factor, β. For injection of 4 MBq/kg [^{18}F]FCH, a frame duration of 1.5 min/bed position with a β-value of 400–550 was required to obtain good image quality.

The accuracy of [^{18}F]FCH PET-CT for staging primary lymph node metastases has been validated, with low sensitivity (43%) and moderate specificity (70%) reported. To examine these results more in-depth, a second study was conducted. In this study, the conventional and novel PET-CT systems were validated based on their ability to accurately detect regional lymph node metastases. This study found large differences in sensitivity and specificity between the PET-CT systems but with almost similar total diagnostic ability. Both studies used histopathology from extended pelvic lymph node dissection as a reference method.

Through a biokinetic and dosimetric study of [^{18}F]PSMA-1007 in patients with prostate cancer, the last study aimed to calculate the absorbed doses and effective dose. The effective dose was calculated to 25 μSv/MBq, corresponding to approximately 8 mSv for a ”standard patient”.

In conclusion, this thesis shows that the reconstruction algorithm BSREM is advantageous over OSEM using [^{18}F]FCH PET-CT, but that the diagnostic accuracy of [^{18}F]FCH PET-CT in detecting pelvic lymph node metastases is not good enough. Furthermore, the thesis shows that the effective dose generated by [^{18}F]PSMA-1007 supporting continued use with the radiopharmaceutical in diagnostic imaging.

Populärvetenskaplig sammanfattning

Risken för att drabbas av åldersrelaterade sjukdomar ökar då vi människor blir äldre och håller oss friskare längre upp i åldrarna. Hjärtkärlsjukdomar är vanligast tätt följt av cancer. Prostatacancer är en av de vanligast förekommande cancersjukdomarna i världen och i Sverige den främsta cancerrelaterade dödsorsaken bland män (1, 2). Tack vare att diagnostik och behandling av cancersjukdomar blivit bättre överlever fler. Idag lever cirka 120 000 män med prostatacancer i Sverige och det är tre gånger fler än för bara 20 år sedan (2).

Diagnostik och stadieindelning av prostatacancer sker bland annat genom bildtagningstekniken positronemissionstomografi (PET) kopplat till datortomografi (DT). Genom denna teknik ges unik information om sjukdomen på molekylär och metabol nivå (3). I mitt forskningsarbete har jag utvärderat ny teknik inom PET-CT vid undersökning av prostatacancer ur olika aspekter. Detta har gjorts genom att vi har sökt de mest optimala inställningarna för undersökningen, testat metodens förmåga att hitta lymfkörtelspridning, samt undersökt fördelningen av och strålningsrisken hos spårämnet som används vid undersökningen. Det är både mjukvaran och hårdvaran i PET-tekniken som utvecklats och förbättrats. Förhoppningen är att detta tillsammans med att nya spårämnen tagits fram ska möjliggöra att mindre metastaser från cancern kan upptäckas med större noggrannhet.

Från en PET-CT undersökning ges en bild över kroppens uppbyggnad och dess funktioner där PET-kameran genererar bilden av funktionen i patientens organ och vävnader. DT-kameran står för bilden som beskriver kroppens uppbyggnad/anatomi. En liten mängd av ett radioaktivt spårämne ges till patienten genom en injektion i blodet. Ett sönderfall av spårämnet sker där små partiklar, positroner, skickas i väg. Positronerna kolliderar med elektroner och fotoner bildas. Dessa integrerar med detektorer i PET-kameran och en bild genereras. Fördelningen av det radioaktiva spårämnet mäts och avbildas genom tekniken. Då PET-CT metoden är kvantitativ kan ett standardiserat upptagsvärde mätas i varje pixel i bilden (3, 4).

Den nya och förbättrade hårdvaran bidrar till en ökad diagnostisk noggrannhet och att mindre strukturer kan åskådliggöras. Bildbehandlingen i mjukvaran har uppdaterats vilken ger ökad kontrast mellan upptag och bakgrund i bilderna samtidigt som det brus som kan störa analysen är betydligt lägre än tidigare. Sammantaget bidrar detta till att mindre strukturer kan upptäckas i en allt större utsträckning (5, 6).

Tidigare var det vanligaste att använda det radioaktiva spårämnet kolin (FCH) vid diagnostik och stadieindelning av prostatacancer. Tyvärr är inte FCH tillräckligt känsligt och specifikt för prostatacancer då FCH också tas upp i andra förändringar än cancer och i andra organ. Så trots att PET-teknikens utveckling möjliggör att

mindre metastaser kan upptäckas hindras diagnostiken av FCH. FCH har därför bytts ut mot det nya radioaktiva spårämnet prostata-specifikt membran antigen (PSMA). PSMA är mer känsligt och specifikt för prostatacancer (7).

Genom studier på den vidareutvecklade och förbättrade hård- och mjukvaran i PET-tekniken och det nyligen introducerade spårämnet PSMA finns förhoppningen om att bättre kunna hjälpa patienter med prostatacancer att få en mer noggrann och korrekt diagnostik och stadieindelning av sjukdomen.

Abbreviations and terms

BPH,	benign prostatic hyperplasia
BSREM,	block sequential regularised expectation maximisation
CNR,	contrast-to-noise ratio
CT,	computed tomography
ePLND,	extended pelvic lymph node dissection
FCH,	[^{18}F]fluorocholine
FDG,	[^{18}F]fluorodeoxyglucose
mpMRI,	multiparametric magnetic resonance imaging
MRI,	magnetic resonance imaging
OSEM,	ordered subset expectation maximisation
PET-CT,	positron emission tomography with computed tomography
PM,	photomultiplier
PSA,	prostate-specific antigen
PSMA,	prostate-specific membrane antigen
RCT,	randomised clinical trials
ROC,	receive operating characteristic
SiPM,	silicon photomultiplier
SPECT,	single-photon emission computed tomography
SUV,	standardised uptake value
TAC,	time-activity curve
TRUS,	trans-rectal ultrasound

Preface

The combination of helping people and technology attracted me to becoming a biomedical laboratory scientist with a specialization in Clinical Physiology (technologist). Nuclear medicine contributed an additional part through the work and knowledge about radioactivity. As I have a natural drive and am curious about several areas, I took my master's degree in in Business Creation and Entrepreneurship in Biomedicine at the University of Gothenburg, where I also completed my bachelor's degree. This education gave me, among other things, a longing to work in and run projects together with other professions. Within my first employment at Linköping University hospital, I began working with PET-CT, quickly becoming a favorite topic. The longing for multidisciplinary research and the curiosity for the functionality of PET-CT systems contributed to me wanting to become a doctoral student. Soon, I had the opportunity to take a combined clinical- and doctoral position at Skåne University Hospital in Malmö and Lunds University within PET-CT and prostate cancer under the supervision of Elin Trägårdh.

Elin had exciting plans around the new PET-CT systems, which interested me as I understood the value of PET-CT examinations in the challenge of diagnosing and choosing the right treatment for patients with prostate cancer. As I worked clinically in parallel with the research, I have conducted some of the included PET-CT examinations on patients with prostate cancer. This has contributed to me being provided with skills in this field.

This thesis was carried out within the PET Research in Skåne (PETRiS) research group, Faculty of Medicine, Lund University, and the Department of Clinical Physiology and Nuclear Medicine and the Department of Radiation Physics, Skåne University Hospital. The studies were founded by ALF Medical Faculty grants at Lund University, Kunt and Alice Wallenberg Foundation and the Swedish Prostate Cancer Foundation, and Region Skåne. The travel grants were funded by the Scandinavian Society of Clinical Physiology and Nuclear Medicine and the Swedish Association for Nuclear Medicine.

Introduction

The main subject of this thesis is to evaluate various aspects of PET-CT imaging when examining patients with prostate cancer.

Prostate cancer is the most common cancer type in men worldwide, and accounts in Sweden today for about 30% of all newly diagnosed cancer cases among men. In 2019, prostate cancer was the form of cancer that caused the most deaths among men in Sweden (1, 2, 8). As prostate cancer primarily affects elderly men and as life expectancy increases worldwide, the prevalence of prostate cancer is expected to increase (2).

Since the 1970s, positron emission tomography (PET) examination has improved the image quality and thereby the opportunity to diagnose diseases (9). The non-invasive imaging technique generates functional data to estimate diseases activity using radiopharmaceuticals. PET combined with computed tomography (CT) provides high-resolution anatomical information and attenuation correction (3, 4). As with all technology, PET-CT is constantly developing and improving, always aiming to improve examination results. Recent updates in the technology have been a shift from conventional photomultiplier (PM)-based PET-CT to a novel silicon-based photomultiplier (SiPM)-based PET-CT, as well as more accurate reconstruction algorithms (6). The development of radiopharmaceuticals is also advancing, with previously well-used [^{18}F]fluorocholine ([^{18}F]FCH) being replaced by [^{18}F]prostate-specific membrane antigen-1007 ([^{18}F]PSMA-1007) in the examination of prostate cancer (10).

This thesis presents feasibility studies addressing various aspects of PET-CT examinations in patients with prostate cancer. At the beginning of this research work in 2017, [^{18}F]FCH PET-CT was used to examine patients with prostate cancer. The machine park at Skåne University Hospital had recently undergone an update, during which the conventional PET-CT systems were replaced by the novel systems. With this update, an optimization study of the method's image reconstruction was performed on behalf of the clinic. Further studies were conducted regarding the diagnostic accuracy of the method [^{18}F]FCH PET-CT, but also on the conventional versus the novel PET-CT systems. Histopathology was used as the reference method. During autumn 2019, further updates of the examination method were performed at the clinic by replacing the [^{18}F]FCH with [^{18}F]PSMA-1007. With this replacement, a biokinetic and dosimetry study of the new radiopharmaceutical was carried out.

Background

The prostate and prostate cancer

The prostate gland

The prostate gland is located below the urinary bladder and in front of the rectum. It encircles the urethra as one single exocrine gland with the size of a walnut (Figure 1). The prostate gland is part of the male reproductive function. During ejaculation smooth muscle contracts and the prostate delivers prostatic fluid into the urethra, of importance for sperm function (11-14). In 1984, an article were published about the anatomy of the prostate where the currently used division of the prostate in its three major histologically and anatomically separated areas was described (15). These areas are defined as the peripheral, central, and transitional zone and are presented in Figure 2.

Prostate cancer, prostatitis, and benign prostatic hyperplasia (BPH) are the most frequently studied conditions affecting the prostate gland. The peripheral zone is the most common site for prostatitis and prostate cancer. The transition zone is often enlarged by BPH, resulting in compression of the urethra, causing impaired voiding. Prostate cancer can also occur in this zone, which may be clinically and biologically different from cancer in the peripheral zone (12-14).

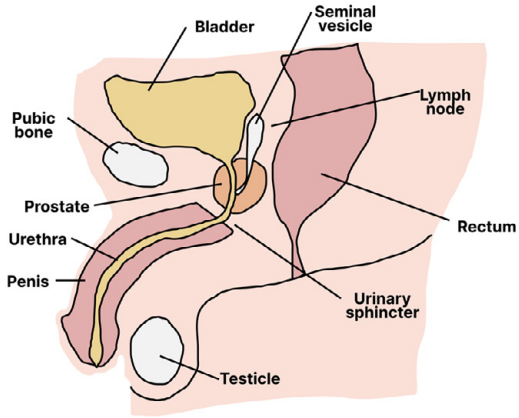

Figure 1. The prostate anatomy.
The prostate gland encircles the urethra and is located below the urinary bladder and in front of the rectum. *The prostate anatomy by William Björsdorff.*

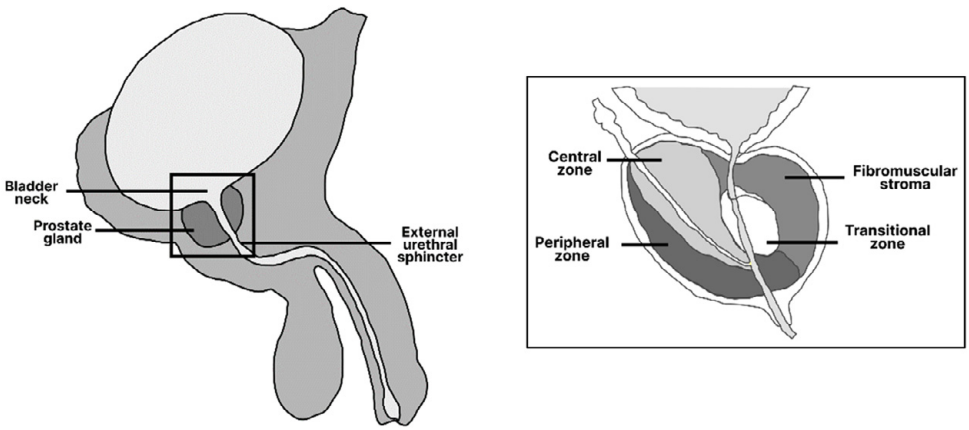

Figure 2. Histological zones within the prostate gland.
The prostate gland is devided in different histological zones. 1) The peropheral zone, 2) The central zone and 3) The transitional zone. *Histological zones by William Björsdorff.*

Prostate cancer

Prostate cancer is one of the most commonly diagnosed cancers in men worldwide and the most common cause of cancer-related death among men in Sweden (1, 2). The number of men who live with diagnosed prostate cancer in Sweden is three times higher today than 20 years ago. This increase is partly due to an increased population with longer life expectancy, earlier diagnosis, and better treatment.

Age, heredity, and external environmental factors are known risk factors for developing prostate cancer. The disease is rarely diagnosed before 40 years old and is not very common before 50 years old. Half of those who die of prostate cancer are greater than 82 years old, and three quarters are over 75 years old. The incidence of the disease varies widely across the world and between different population groups. The variation is believed to be due to a combination of external environmental factors and genetic factors, where it is difficult to define exactly what affects the variation (1, 2). However, studies on the prevention of the onset of prostate cancer using certain diets, vitamins, or selenium have thus far been unsuccessful (16, 17). Heredity is a strong factor in the risk of developing prostate cancer. Sons of men who have prostate cancer are at greater risk of being diagnosed than men without prostate cancer in the family. The risk increases further for brothers of men who have the disease. If prostate cancer is only on the mother's side, the risk of a man contracting prostate cancer does not increase, as long as the mother has not suffered from breast or ovarian cancer (1, 2).

Mortality from prostate cancer decreases with regular prostate-specific antigen (PSA) screening of men between 50 and 70 years old. However, this also leads to overdiagnosis and overtreatment of cancer without clinical significance, which is why the risk does not outweigh the benefits. Therefore, screening is advised against by the National Board of Health and Welfare in Sweden (18). Systematic prostate biopsies in men with slightly elevated PSA values often lead to prostate cancer diagnosis in men who would never have developed symptoms of prostate cancer (2).

Screening studies are underway where magnetic resonance imaging (MRI) may play an important role as a triage test to avoid unnecessary prostate biopsies. Recently, the value of combining MRI and the Stockholm3-test, which is a combination of clinical information and a blood test of different proteins and a gene panel, was reported (19, 20). From this study, the first results show that the combination of MRI and the Stockholm3 test increases the precision of finding treatment-requiring prostate cancer. The results also show that overdiagnosis decreases, and fewer men need to undergo biopsy tests (21).

Currently, opportunistic PSA testing takes up large healthcare resources, and incomplete information about this is released. To create standardization and streamlining of prostate cancer testing, pilot projects with organized prostate cancer testing have been started in Region Skåne and the Västra Götaland region, where all

men between 50 and 74 years old in these regions will be invited for a PSA test. More regions will join as time goes on (2).

Death associated with prostate cancer is caused by metastatic disease, where the primary site of metastases often is in pelvic lymph nodes. Secondary sites for metastases are in bones. In the late and advanced stages of the disease, metastases also occur at other sites such as the lungs and liver (22).

Diagnostic methods

To find the best treatment for a patient with prostate cancer, information about the characteristic of the tumour and the stage of the disease are required. Prostate cancer is diagnosed through pathological examination of biopsies, digital rectal examination, and increased PSA value. A majority of prostate cancers is multifocal which is why a combination of diagnostic methods and imaging modalities is required to gather sufficient information about the extent of the disease (2).

Primary diagnosis

A simple blood test of PSA is commonly used first in the diagnostic setup. PSA is a protein in semen, secreted from the prostate, and it is needed for normal sperm function (23). There is a small natural leakage of PSA into the bloodstream. The PSA value increases with cancer, prostatitis, and BPH. The ratio between the free form of PSA (not bound to other proteins in the blood) and the total PSA indicates if a moderately elevated level of PSA is due to prostate cancer or BPH (24).

The prostate biopsies guided by trans-rectal ultrasound (TRUS) are assessed based on the Gleason score classification system (1, 2, 25, 26). The patterns of cells in the histological preparations are estimated and graded on a 10-point scale where a higher number indicates more aggressive disease. The degree of the most common growth pattern is added to the second most common or the worst growth pattern in the preparation, which is summed up to the Gleason score for the entire histological preparation. Modifications to the Gleason score have been done over the years and the most recent resulted in the International Society of Urological Pathology (ISUP)-grading where the Gleason score become grouped in a 5-point scale (Table 1 and Figure 3) (1, 2, 25-28). In the Swedish national guidelines for prostate cancer, a Gleason score of ≤6 is categorized as low risk and 3+4 as intermediate risk. Gleason scores 4+3 found in half of the systematic biopsies or 4+3 found in targeted biopsies the disease is classified as high risk. Gleason score 8 is also categorized as high risk and severe high-risk prostate cancer presents a Gleason score of 9–10 (1, 2).

Table 1. Gleason score and ISUP-grading.
The Gleason score in relation to the ISUP-grading from the consensus conference held by the International Society of Urological Pathology (ISUP) 2014.

Gleason score	ISUP-grade	
≤6	1	Low risk
3+4=7	2	Intermediate risk
4+3=7	3	High risk if 4+3 are represented in half of the systematic biopsies, alternatively represented in targeted biopsies
8	4	High risk
9–10	5	Severe high risk

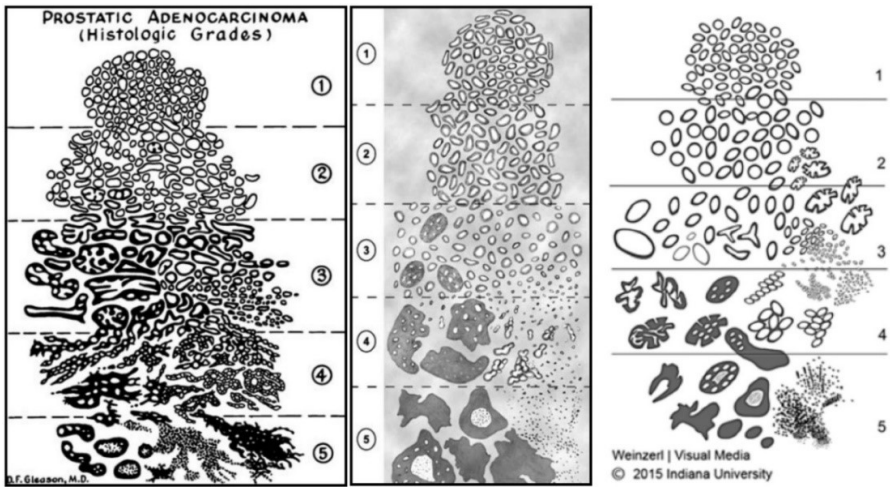

Figure 3. Gleason score.
Illustrations of histological preparations and different patterns. On the left is the original drawings by Gleason in 1966. In the middle presents the Gleason score modification in 2005. To the right, the changes were made at the ISUP conference in 2015. *Image used with permission from Regionala cancercetrum* (2).

Staging

The TNM staging system is the international gold standard to stage cancers (Table 2). The system has some limitations due to interobserver variation when image examination is interpreted (2).

Tumour (T) specifies the local stage of the tumour, which is assessed by palpation from the rectum and TRUS. According to European guidelines, digital rectal examination findings are advocated before TRUS (1). The regional nodes (N) are best assessed by pelvic lymph node dissection (PLND) but today also by MRI and CT. However, MRI and CT have low sensitivity and specificity for detecting of regional metastases in lymph nodes. [^{18}F]FCH PET-CT, on the other hand, has higher sensitivity and specificity. For [^{18}F]PSMA PET-CT, the diagnostic accuracy increases further, but so far there is no evidence of how the treatment should be affected in PET findings that give rise to suspicion of lymph node metastasis. Distant metastasis (M) of prostate cancer is dominated by skeletal metastases and

are primarily detected by bone scintigraphy or PET-CT but may also be detected by MRI or CT (1, 2). See below for more information about the different imaging modalities.

Table 2. TNM classification.
TNM-classification due to Union for International Cancer Control (UICC) 2017.

T-stage, Primary Tumour	
T0	No primary tumour
Tx	The primary tumour is not assessed
T1	The cancer is not palpable or detected
T2	The cancer is palpable or detected within the prostate gland
T3	The cancer is palpable or detected outside the prostate gland
T4	Cancer grows into nearby structures
N-stage, Regional (pelvic) Lymph Nodes	
N0	No regional lymph node metastasis
Nx	The regional lymph node is not assessed
N1	The regional lymph node is detected
M-stage, Distant Metastasis	
M0	No distant metastasis is detected
M1	Distant metastasis is detected

Table 3. Division of risk groups in prostate cancer.
The division of risk groups is based on systematic biopsies (1, 2).

Division of risk groups	
Low risk	T1–T2a, Gleason score ≤6 and PSA ≤10µg/l
Intermediate risk	T2b and/or Gleason score 7 and/or PSA 10–19.9 µg/l
High risk	T2c–T3 and/or Gleason score 8–10 or widespread pattern of 4+3=7, and/or PSA ≥20µg/l

The prostate cancer prognosis is based upon the TNM classification, PSA-value, and Gleason score, from where risk grouping is done (Table 3).

Choice of treatment

When choosing treatment, the patient's wishes must weigh heavily. Information on the possible pros and cons of the various treatments should be provided, including any side effects that may occur. Before curative treatment, an assessment is made of the function in the lower urinary tract and the intestine before offering surgery or radiation therapy. The same applies to erectile function and how important it is for the individual patient to preserve it. Patients with very low- or low-risk prostate cancer are recommended active surveillance, where curative treatment may become relevant later. Active surveillance involves the follow-up of untreated prostate cancer if the aim is to provide curative treatment if the disease progresses. In the

case of a life expectancy of fewer than 10 years, or in the case of comorbidity where the cancer is not expected to contribute to premature death, watchful waiting is recommended and with palliative treatment, commonly hormonal treatment, when symptoms occur. Treatment options for intermediate-risk prostate cancer are radiation therapy or radical prostatectomy if the life expectancy is more than 10–15 years (1, 2). Radical prostatectomy is done either with open surgery, laparoscopic technique, or robot-assisted laparoscopic prostatectomy. The prostatectomy techniques can be combined with extended pelvic lymph node dissection, ePLND (29). External radiation therapy or low-dose brachytherapy can be used with curative intent. In the use of low-dose brachytherapy, radioactive seeds are placed in the prostate using a perineal approach under anaesthesia. The local radiation dose is high in the tumour area but low in surrounding organs. Patients with high-risk prostate cancer may also be eligible for curative treatment based on life expectancy. This is discussed at a multidisciplinary conference. Patients with high-risk prostate cancer and clinical tumour stage cT1–2 may be eligible for either radiation therapy combined with hormone therapy or radical prostatectomy. For locally advanced prostate cancer at stage cT3, radiation therapy is combined with hormone therapy or randomized between surgery or radiotherapy in the SPCG-15 study (30, 31). Treatment for those patients with very high-risk prostate cancer is like the treatment for patients with high-risk prostate cancer after staging for metastases. In patients with stage cT4, radiation therapy in combination with hormone therapy is recommended (1, 2). To calculate the risk assessment of positive lymph node and biochemical recurrence, nomograms, such as D'Amico (32, 33), are used by entering the Gleason score, clinical stage, and PSA. The conventional imaging modalities to predict lymph node involvement were bone scintigraphy and CT scan, but PET-CT and MRI are used more often today (2, 29).

Biochemical recurrence

Within 10 years of definitive treatment of prostate cancer, biochemical recurrence, increased PSA values occurs in 20–40% of patients. Within those, 10–70% of the patients get bone metastases within 5 years. Biochemical recurrence, defined as measurable PSA in blood at <0.20 ng/ml with a subsequent confirmatory value, is usually the first sign that the prostate cancer has recurred locally or metastasized after radical prostatectomy. A different definition of recurrence is used after radiotherapy according to the Phoenix criteria with PSA nadir, the lowest PSA value after radiotherapy, plus 2.0 ng/ml (34). The PSA value doubling time, Gleason score, and pathological stage are significant parameters for whether biochemical recurrence will generate metastases. PSMA radioligands PET-CT has shown high sensitivity and specificity in detecting remaining cancer in biochemical recurrence after prostatectomy and radiation treatment and is recommended in several guidelines. Other imaging techniques do not provide relevant information (1, 2, 35).

Positron emission tomography-computed tomography

Positron emission tomography combined with computed tomography (PET-CT) is a non-invasive nuclear medicine imaging technique that generates functional and anatomical images in one session. One gantry with two scanners and a patient bed makes up the multimodality system. To produce functional images, PET uses molecules labelled with radiotracers, also called radiopharmaceuticals, which contains biologically active molecules labelled with a non-stable radioactive nuclide. Depending on the organ or metabolic process of interest the biological molecules are changed to resemble the physiological substance. CT uses x-ray to map the anatomy within the body and it also assists with attenuation correction of the PET image. Like other nuclear medicine techniques, PET-CT can detect pathophysiological changes at an early stage before the symptoms are clinically evident and anatomical changes have occurred (36). PET-CT is mostly used within oncology to assess the stage and recurrence of the disease and evaluate treatment of the disease. It is also used in cardiology, neurology, and different inflammatory, and infectious diseases (36-40). Through the fused PET-CT images, the course of the disease can be followed.

Radiopharmaceuticals

Radiopharmaceuticals are used to visualise and examine the function within an organism at PET-CT. Radiopharmaceuticals are biologically active "carrier molecules" (pharmaceuticals) with either one atom replaced with a radioactive nuclide (e.g., flourine-18) or a radionuclide attached to a molecule/peptide (e.g., galluim-68). To assess different cancer diseases fluorine-18 (^{18}F), carbon-11-methyl (^{11}C) and gallium-68 (^{68}Ga) are some of the most important radionuclides, and (^{18}F) – with its 109.7 min half-life – is most used (41). Different radiopharmaceuticals are used depending on the organ or metabolic process to be examined. In general, [^{18}F]fluorodeoxyglucose ([^{18}F]FDG) is the most frequently used radiopharmaceutical, but for examination of prostate cancer acetate, sodium fluoride (NaF), choline, or prostate-specific membrane antigen (PSMA) are mostly used (41, 42).

[^{18}F]fluorodeoxyglucose

[^{18}F]FDG is the most common PET radiopharmaceutical. It is a glucose analogue that enters the cell using glucose transporters in the cell membrane. [^{18}F]FDG is not metabolised as glucose molecules; the [^{18}F]FDG will, therefore, be trapped in the cell, which makes it possible to image (43, 44). Uptake of [^{18}F]FDG is detected in malignant tumours, inflammations, and infections (36-38, 40). It is also used to examine the presence of dementia, but here it is the lack of uptake of [^{18}F]FDG that is measured (40, 45). Many cancers are characterized by rapidly dividing cells and upregulated glucose metabolism. However, prostate cancer often has a low

metabolic activity, which might mean that [^{18}F]FDG will not be useful (35). Also, [^{18}F]FDG is excreted in the urine, and thus lesions near the bladder can be covered (41, 44). In patients with aggressive primary tumours and with biochemical failure, [^{18}F]FDG may be useful for staging and site localization of disease in some patients with prostate cancer (42, 46).

Acetate

Cells use acetate in their energy metabolism, and radiolabelled acetate reflects the lipid metabolism. [^{11}C]acetate PET-CT is routinely used for primary diagnosis, staging, and therapy evaluation of patients with prostate cancer. Malignant accumulation of [^{11}C]acetate is also a strong predictor of survival in patients with biochemical recurrance after completed prostatectomy (47-50). Studies have shown that [^{11}C]acetate performs worse than [^{68}Ga]PSMA-11 in the detection of suspected and established lymph node metastases and bone metastases (50). In larger patient groups, [^{11}C]acetate becomes difficult to use as the half-life of (^{11}C) is relatively short, 20 min. In addition, only a small amount is produced at a time, which is also expensive for larger patient groups.

Sodium fluoride

[^{18}F]NaF PET-CT provides information about osteoblastic activity and bone remodelling, where the response to treatment in patients with prostate cancer metastases is assessed through the examination method. The method has many similarities with bone scintigraphy which is performed using technetium-99m-labelled bisphosphonate compound and planar bone scintigraphy with or without single-photon emission computed tomography (SPECT). However, [^{18}F]NaF is superior to bone scintigraphy as the soft tissue clearance is faster for [^{18}F]NaF as well as having a greater bone uptake, i.e., shorter examination time and higher bone-to-background contrast. However, bone scintigraphy is more easily accessible (46, 51).

Choline

Trapping of choline occurs in the formation of phospholipids in the cell membrane of the tumour and choline kinase is upregulated in malignant tumours. Radiolabelled choline is trapped to a greater extent in cancer cells and is thus a suitable radiotracer that reflects cell membrane turnover in the body (35, 41, 44, 52). [^{11}C]choline or [^{18}F]fluorocholine ([^{18}F]FCH) are widely used in the diagnosis of prostate cancer and its recurrence, but also in monitoring the effect of therapy (Figure 4) (1, 40, 46). The specificity is higher for [^{18}F]FCH than for [^{11}C]choline for detection of local lymph nodes and distant metastases of prostate cancer (35, 40).

Choline PET-CT is not considered to reach clinically acceptable diagnostic accuracy for detecting lymph node metastases due to low sensitivity and moderate specificity (1, 53, 54). It has, therefore, been replaced by PSMA in many

institutions. Choline may have a potential role in prostate cancer cases that are negative for PSMA (46).

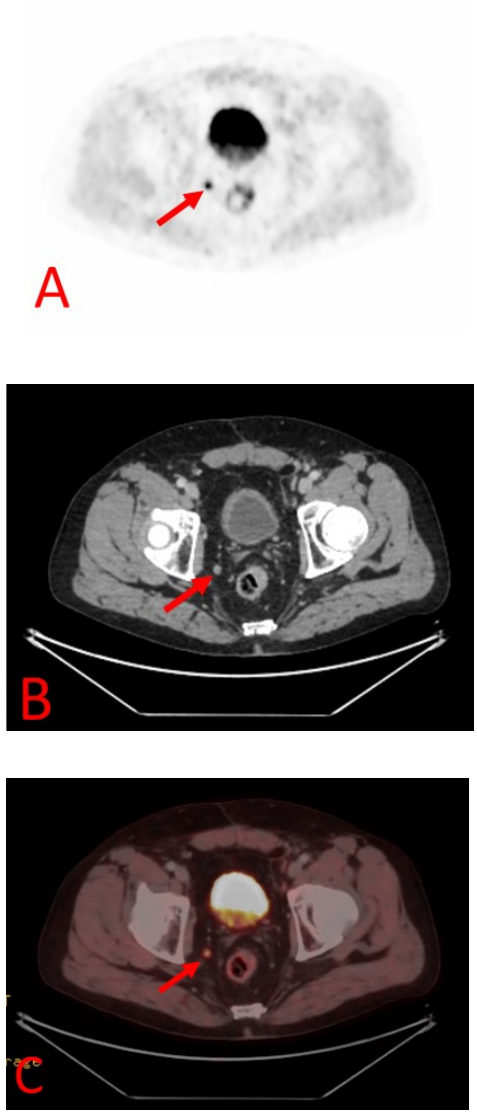

Figure 4. [^{18}F]FCH PET-CT
Pelvic transversal images in a patient with high-risk prostate cancer undergoing [^{18}F]FCH PET-CT. The arrow points to the [^{18}F]FCH uptake in a pelvic lymph node. Image A represents the PET image, B the CT image, and C the fused PET-CT image.

Prostate-specific membrane antigen

In prostate cancer, the expression of PSMA increases 100- to 1000 times on the surface of prostatic cancer cells compared to normal tissue. PSMA is a transmembrane glycoprotein and is naturally expressed in the cytosol of normal prostatic tissue. However, PSMA is also expressed in non-prostatic malignancies, sarcoidosis, and benign bone diseases, contributing to false-positive findings (1, 7, 46, 50, 55).

PSMA-ligand PET-CT is used to examine patients with prostate cancer for initial staging or to identify recurrence sites (Figure 5) (56). [^{68}Ga]- and [^{18}F]-labelled PSMA PET-CT is considered to reach clinically acceptable diagnostic accuracy for detection of lymph node metastases due to its excellent contrast-to-noise ratio (CNR) that generates higher sensitivity in comparison to radiolabelled choline (1, 55, 57). The performance of [^{68}Ga]PSMA-11 versus [^{18}F]PSMA-1007 has proven to be similar. However, [^{18}F]PSMA-1007 provides more non-specific uptake into the skeleton but a theoretical better image quality than [^{68}Ga]PSMA-11 (57, 58). Another advantage of [^{18}F]PSMA-1007 is that it is not excreted in the urine like [^{68}Ga]PSMA-11, which introduces a risk of obscuring small uptake in the vicinity of the bladder (58).

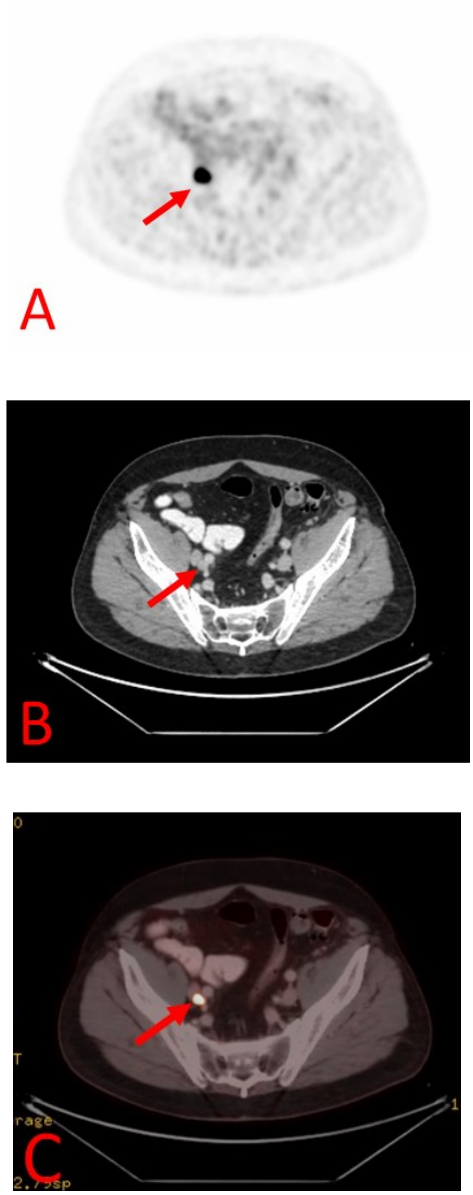

Figure 5. [^{18}F]PSMA-1007 PET-CT.
Pelvic transversal images in a patient with high-risk prostate cancer undergoing [^{18}F]PSMA-1007 PET-CT. The arrow points to the [^{18}F]PSMA-1007 uptake in an iliac lymph node. Image A represents the PET image, B the CT image, and C the fused PET-CT image.

Principles of PET

The radiopharmaceuticals used in PET examinations are administrated via intravenous injection into the patient's blood. The tracer is distributed in the body to portray the process of interest after a known time. For example, uptake from the radiopharmaceutical [^{18}F]FCH in prostate (but also in other organs) and lymph nodes in prostate cancer can be seen in the PET image after a 60-min accumulation time. Positively charged electrons, positrons, are emitted from the radioactive nuclide. The positron annihilates with an electron producing two high-energy photons (E = 511 keV) travelling in approximately opposite directions. The annihilation is usually located within a small distance, a tenth of a millimetre, from the decaying atom. The PET image is based on quantitative information about the detection of the photons. When two photons emitted between the detectors are detected in a short time window, the detection is called a coincidence event and paired as a true coincidence pair. In general, the number of detected coincidence events will be proportional to the number of radionuclides in the line of response. Based on this statement, coincidence events are processed to reconstruct the image. Random and scattered coincidence can also occur, which can be detected and classed as false coincidence pairs. In a random coincidence, only one photon from each of two decaying atoms is detected within the time window while their counterparts are lost to the system. A scattered, Compton, coincidence occurs when a photon loses some of its energy and change its direction on the way to the detectors (3, 4).

The high energy photon is absorbed in the detector, interacting with the scintillating crystals. Here the energy of the photons is reduced to lower energy. Coupled to the crystals are either photomultiplier (PM) tubes or the newer generation silicon-based photomultipliers (SiPM), which measure the photon energy. SiPM has the advantage of requiring less voltage and being electromagnetically less sensitive than PM-tubes (6, 59, 60). PET-CT systems with SiPM have been shown to produce higher image quality and more sensitivity than systems without SiPM (59, 61, 62).

The system localizes the annihilation position, and the measurements are organised through a histogram matrix from which image reconstruction occurs to format the PET image (3, 4).

Reconstruction algorithms

Image reconstruction is the process where collected raw data forms the PET image. Reconstruction of PET images is done by using the coincidence events detected to provide cross-sectional images of the radiopharmaceutical distribution (3, 4).

Image reconstruction algorithms are based on iterative methods in modern PET-CT scanners. In iterative reconstructions, estimates are made of an image in different steps. These estimates are repeated until the image best represents the real object. A

common reconstruction algorithm is called ordered subset expectation maximisation (OSEM) (3, 4, 40).

The resolution in the image increases with an increased number of iterations, which is why small objects require more iterations. Along with an increased number of iterations, the noise also increases. A post-reconstruction smoothing filter is used to regulate the noise. However, the filter reduces the resolution of the image. A balance between resolution and noise is required when choosing the number of iterations and post-filters in the reconstruction (3, 4).

By including calculations of neighbouring voxels, the development of iterative reconstruction has taken further steps forward. This is the basis for block sequential regularised expectation maximisation (BSREM) (6). One commercial application of BSREM is called Q.Clear (GE Healthcare, Milwaukee, WI, USA) (63). Compared to OSEM, BSREM can maintain a low noise level as the number of iterations increases. This reduces the need of "stopping early" as a strategy for noise control and allow for more iterations while keeping the noise level at acceptable levels. BSREM has a penalty factor β, which suppress the noise based on user input. However, the resolution is reduced when noise is suppressed (6).

Through optimizing the reconstruction, safer results with fewer uncertain lesions can be ensured, and image assessment becomes more efficient. This thesis presents an optimization study of the novel reconstruction algorithm BSREM versus the OSEM algorithm (64). Studies have shown better quantitative accuracy of standardised uptake value (SUV), especially in small lesions when using BSREM when OSEM and BSREM have been compared (5, 63, 65-70).

Quantification in PET imaging

The radiopharmaceutical accumulation can be quantified by both PET and SPECT; however, it is not done as often with SPECT. In this way, PET has an advantage over other nuclear medicine techniques by quantifying radiopharmaceutical accumulation (3, 4). The quantification is mostly expressed as the SUV where the activity concentration in relation to the amount of activity injected and the patient's body weight is measured (Equation 1). However, the quantification is affected by some deficiency in the PET technology, such as the spatial resolution, spill-in effect, and reconstruction algorithm, which can cause difficulties in detecting small lesions. The quantification is also affected by biological effects, such as body size measurement and blood glucose concentration. These technological and biological factors, among others, highly impact the SUV of lesion size, volume, and contrast recovery. Although SUV is used to quantify a PET examination, SUV will differ between examination on different PET-scanners and from one day to another, which represents a problem in clinical and research imaging (71).

$$\text{SUV} = \frac{\text{Activity concentration in tissue}}{\text{Injected activity / Body mass}}$$ Equation 1 (71)

Other imaging modalities

Bone scintigraphy and SPECT

Bone scintigraphy is a commonly used method for detecting bone metastases by showing the osteoblastic activity in the bone (72, 73). By binding the radionuclide technetium-99m (^{99m}Tc) to a bisphosphonate compound, hydroxymethylene diphosphonate as an example, [^{99m}Tc]Tc-HDP, the osteoblastic activity can be followed. Increased osteoblast activity thus results in increased nuclide uptake (72, 73). Figure 6 shows the two-dimensional planar images of patients with prostate cancer. Planar bone scintigraphy can be combined with SPECT-CT over a certain area of the body, often the pelvis. The 3D SPECT images combined with a CT can identify, for example, metastases hidden by the activity in the bladder in the planar images. It can also increase the diagnostic certainty, for example, better differentiate an uptake into a degenerative or metastatic lesion. The sensitivity of planar bone scintigraphy is limited by the anatomical location of the lesion. Together with SPECT-CT, the sensitivity increases slightly. In contrast, (^{18}F)-PET is more sensitive to detecting benign and malignant bone lesions (46, 74).

Figure 6. [^{99m}Tc]Tc-HDP Bone scintigraphy.
High-risk prostate cancer patient with skeletal metastasis in the left femur.

Computed tomography

CT provides detailed anatomical cross-sectional images through x-rays. An x-ray tube and detector are connected opposite each other and rotate around the continuously moving patient table at the same time as the x-rays are emitted and detected. The density and permeability of the organs affect the number of x-rays absorbed in the various organs and the amount of x-ray that can integrate with the detector. The CT technology acquires images for every 360 degrees, allowing highly detailed images of the body's anatomy to be generated in three dimensions. Injuries and diseases of organs can be detected, localized, and classified with CT. When examining with CT, an intravenous and/or oral contrast agent is usually used to enhance the contrast between the different structures of the body. In combination with PET, CT contributes with anatomical information and data for attenuation correction of the PET-CT image. Attenuation correction is applied to overcome quantitative imaging errors from different types of coincidence, such as missing photons due to attenuation in random coincidence and scattered photons in Compton coincidence (75).

The imaging modality is recommended in the Swedish care programme for prostate cancer for staging patients with intermediate- and high-risk prostate cancer (2). CT can provide information about regional and distant metastases where pelvic lymph nodes metastases and bone metastases are most common in prostate cancer. Information about the size and shape of lymph nodes can be provided, where enlarged lymph nodes indicate possible lymph node metastases. Sclerotic lesions in the bone may indicate bone metastases. Metastases detected in the lungs and liver occur mainly in the later stages of the disease (22, 76, 77).

When comparing PSMA PET-CT and conventional imaging (defined as combined findings of CT and bone scintigraphy) in detecting pelvic lymph node metastases in patients with high-risk prostate cancer, PSMA PET-CT proved to have superior diagnostic accuracy to conventional imaging (46, 78, 79). In one of the studies, PSMA PET-CT had a 27% absolute higher AUC for accuracy than conventional imaging. This was also reflected for sensitivity (38% versus 85% for conventional image and PSMA PET-CT, respectively) and specificity (91% versus 98%, conventional image and PSMA PET-CT, respectively) (78).

Magnetic resonance imaging

Magnetic resonance imaging (MRI) produces images through essentially three parts: a strong magnetic field that affects the hydrogen atoms in the body; gradient magnets that are rapidly turned on and off (creating small local variations and enabling visualization of all planes in the body); and the third part that contains components that transmit and receive radio-frequency pulses (80). With MRI, injuries and diseases of organs and certain parts of the skeleton can be detected,

localized, and classified. Both anatomical and functional sequences are produced without using ionizing radiation. Detailed anatomic assessment and soft-tissue resolution of the prostate is generated by multiparametric (mp) MRI (46). mpMRI has a higher sensitivity for clinically significant prostate cancers than TRUS, bone scintigraphy, CT, and PET-CT. However, the specificity is low for mpMRI; this is why an image-guided biopsy is important in assessing prostate cancer. (81-83).

Trans-rectal ultrasound

TRUS is a cornerstone of prostate cancer diagnosis and is used in biopsy in prostate cancer (1, 84). The prostate can be imaged by inserting an ultrasound probe into the rectum. Biopsies are then taken with a needle which is passed through a channel on the ultrasound probe. Prostate biopsies guided by TRUS with or without previous MRI provide further important information on the diagnosis and characterization of the primary tumour. Biopsy of the prostate is either done blindly based on a schedule – which is called systematic biopsies, – or through targeted biopsies when biopsies are taken against a cancer-suspected area designated by MRI (1, 84, 85).

Biokinetics and dosimetry

Both in diagnostic and therapeutical nuclear medicine, knowledge about the distribution of the tracer in the body is important. This knowledge and understanding can be obtained through kinetic and dosimetry studies. Biokinetics studies examine how the radiopharmaceutical is distributed in the body over time, and based on this result, the biological half-life of the radiopharmaceutical in different organs is calculated. In dosimetry studies, it is investigated how much energy from the radionuclide is absorbed in the organs, i.e., how dangerous a radionuclide can potentially be for different organs and the whole body. This is presented in the absorbed dose and effective dose. The organs are affected both by the radiation from the amount of radionuclide the organ itself absorbs, so-called self-dose, and by radiation from other nearby organs that have taken up the radionuclide, cross-dose, which is also included in the dosimetry calculation (4, 86, 87).

The distribution of a radiopharmaceutical can be monitored using quantitative measurement techniques, such as SPECT and PET imaging techniques; external non-imaging radiation monitoring with NaI probe; tissue samples from blood and biopsies; and excretion counts in urine and faces. The measurements are repeated to be able to follow the distribution of activity in the body during a certain time after administration. Organs that absorbed a significant amount of radiopharmaceuticals must be followed (87).

Based on the measured values, time-activity curves (TACs) can be created for each organ directly. However, no TACs are given for the organ on which no measurement has been made. To obtain these measurement values, a compartment model can be created, which has the advantage that it is possible to add and estimate the activity in organs, compartments on which no measurement has been made. The model describes how the activity is carried from one compartment to another through a known tissue, such as blood. Based on the compartment model, TACs for the compartments in the model can be created and thereby given mean values that better represent a population (87).

One method used to calculate the radiation risk in nuclear medicine examinations is the dosimetry scheme Medical Internal Radiation Dose (MIRD) (86, 87). Using the method, the absorbed dose to the organs and the effective dose for the whole body can be calculated.

When using TAC, it is important to remember that the calculation is based on the small population included in the study. To calculate radiation dose, factors developed using stylized computer phantoms are used. This, in turn, means that the calculated radiation dose applies as an average of a large population. Therefore, care should be taken to use the value when estimating the dose to an individual patient.

Rationale

Examinations with PET-CT system with PET and CT modalities combined into a single device – has been used since the introduction of the system in 1991 by Townsend and Nutt (9).

To increase the performance and accuracy to detect the location of the positron-emission in the patient, the PET-CT hardware has been upgraded in terms of the number of detectors, scintillator crystals and photodetector combinations. Software improvement have mostly addressed data processing, reconstruction algorithms, and image analysis (9, 59, 60, 62, 63, 65). The method is further improved by developing radiopharmaceuticals that are more specific for a certain disease.

At the beginning of the research project in 2017, the [^{18}F]FCH PET-CT examination method had to be optimized for the new SiPM-based PET-CT systems since the systems were recently installed then. The [^{18}F]FCH PET-CT examination method was used to a potential greater extent in the population in Skåne than in other Swedish hospitals. Therefore, the knowledge of the examination method's accuracy, in its entirety but also differences between the conventional and novel PET-CT systems, was of great importance. The new radiopharmaceutical [^{18}F]PSMA-1007 was introduced at Skåne University Hospital in 2019. The knowledge about the biokinetic and dosimetry for this new radiopharmaceutical was limited, and, therefore further investigation are needed.

This dissertation provides examples of studies that are carried out in connection with the installation of new PET-CT equipment and when new pharmaceuticals are introduced. The dissertation is important to 1) optimize the use of the examination method [^{18}F]FCH PET-CT on the novel PET-CT system based on image quality and assessment, 2 and 3) understand the diagnostic performance of [^{18}F]FCH PET-CT, also between different PET-CT systems, and 4) provide knowledge about the biokinetics and dosimetry of [^{18}F]PSMA-1007.

Aims of the studies

The overreaching aim of this thesis was to, for patients with prostate cancer, evaluate [^{18}F]FCH with the conventional PM-based and the new SiPM-based PET platform and to investigate the new radiopharmaceutical [^{18}F]PSMA-1007. This was done through optimization of protocols in the new PET-CT for [^{18}F]FCH, studies of the diagnostic accuracy for [^{18}F]FCH in conventional and novel PET-CT systems, and biokinetic and dosimetry study of the novel radiopharmaceutical [^{18}F]PSMA-1007.

Specific aims

Paper I The aim was to evaluate image quality and diagnostic performance of different reconstruction protocols for patients with prostate cancer being examined with [^{18}F]FCH on the novel SiPM-based PET-CT.

Paper II The aim was to assess the accuracy of detecting regional lymph node metastases using [^{18}F]FCH PET-CT. Histopathology from ePLND was used as a reference method.

Paper III The aim was to compare the accuracy of detecting regional lymph node metastases between conventional PM-based and novel SiPM-based PET-CT technology using [^{18}F]FCH. Histopathology from ePLND was used as a reference method.

Paper IV This study aimed to investigate the whole body-biokinetic and radiation dosimetry of [^{18}F]PSMA-1007 in patients with prostate cancer.

Materials and methods

All patients in this thesis had prostate cancer and were referred for PET-CT examination ([^{18}F]FCH or [^{18}F]PSMA-1007) at the Department of Clinical Physiology and Nuclear Medicine, Skåne University Hospital, Sweden, starting in 2017.

Data collection procedure

All studies are based on data from PET-CT examinations and patients' medical records. The PET-CT examinations were performed similarly through the four studies with the difference in when [^{18}F]FCH versus [^{18}F]PSMA-1007 was used. Three different PET-CT systems were used, the SiPM-based GE Discovery MI PET-CT (GE Healthcare, Milwaukee, WI, USA), and the two conventional PM-based PET-CT systems GE Discovery 690 PET-CT (GE Healthcare, Milwaukee, WI, USA), and Philips Gemini TF (Philips Healthcare, Cleveland, OH, USA). OSEM and BSREM with different β-values and frame durations were used as reconstructions algorithms.

The patients in the optimization (Paper I) and both studies on diagnostic accuracy (Paper II and III) were fasting a minimum of 4 h before the intravenous injection of 4 MBq/kg [^{18}F]FCH. The PET-CT examination was performed after an accumulation time of 1 h after the injection. The images were acquired from the upper thigh to the base of the skull with a frame duration of 2.0 min per bed position. A diagnostic CT was also obtained from the upper thigh to the base of the skull. The patients in studies II and III underwent ePLND after the PET-CT examination.

In the biokinetic study (Paper IV), a first blood sample was taken just before the intravenous administration of 4 MBq/kg [^{18}F]PSMA-1007. The intravenous injection was given 3 min before the first of eight PET-CT scans was started. The remaining seven PET-CT scans were performed 10, 20, 30, 60, 120, 210, and 330 min after injection. Blood samples were taken just before the scans started and all urine during the day was collected. Figure 7 describes the duration time of the different scans. Regions of interest were drawn in the PET-CT images to segment the organs to determine the amount of activity in the organs.

Blood sample	Scan p.i	Time (sec) per bed position (10 bed positions)										CT protocols
		Over the thigh		Rest of the body								
1	3 min	15	15	30	30	30	30	30	30	30	30	120kV/30-160mA
2	10 min	15	15	30	30	30	30	30	30	30	30	120kV/30-160mA
3	20 min	15	15	30	30	30	30	30	30	30	30	120kV/30-160mA
4	30 min	15	15	30	30	30	30	30	30	30	30	120kV/30-160mA
5	60 min	60	60	120	120	120	120	120	120	120	120	120kV/30-160mA
6	120 min	120	120	120	120	120	120	120	120	120	120	120kV/30-160mA
7	210 min	60	60	120	120	120	120	120	120	120	120	120kV/30-160mA
8	330 min	90	90	210	210	210	210	210	210	210	210	120kV/30-160mA

Figure 7. Examination procedure in the biokinetic study
The examination procedure for the pateints included in the biokinetic study. The scanning 120 min p.i is the diagnostic examination. Blood samples were collected in connection with each scan. Urine was collected in separate bottles during the day until the next morning. P.i = Post injection.

Overview of the thesis

Table 4 summarizes the four studies included in this thesis.

Table 4. Overview of the four studies in this thesis.
BSREM = block sequential regularisation expectation maximisation; ePLND = extended pelvic lymph node dissection; FCH = [^{18}F]fluorocholine; PET-CT = positron emission tomography with computed tomography; PM = photomultiplier; PSMA = [^{18}F]prostate-specific membrane antigen-1007; ROC = receiver operating characteristics; SiPM = Silicon photomultiplier

	Paper I Optimization study	Paper II Diagnostic accuracy study	Paper III Diagnostic accuracy study	Paper IV Biokinetic study
Aims	To compare image quality and diagnostic performance of different reconstruction protocols for patients with prostate cancer being examined with FCH on a SiPM-based PET-CT	To assess the accuracy of detecting regional lymph node metastases using FCH PET/CT. Histopathology from ePLND was used as the reference method.	To compare the accuracy of detecting regional lymph node metastases between conventional PM-based and novel SiPM-based PET-CT technology using FCH. Histopathology from ePLND was used as the reference method.	To investigate the whole body-distribution and radiation dosimetry of PSMA in patients with prostate cancer.
Number of participants	13	252	177	12
PET-CT system	GE Discovery MI	GE Discovery MI Philips Gemini TF GE Discovery 690	GE Discovery MI Philips Gemini TF	GE Discovery MI
Reconstruction algorithm	BSREM OSEM	BSREM	BSREM	BSREM
Data	Image analysis, assessment and interpretation of images	Absence/presence of suspected lymph node metastases, PET-CT vs. ePLND	Absence/presence of suspected lymph node metastases, PET-CT vs. ePLND	Biokinetics and Radiation dosimetry
Data collection methods	PET-CT imaging data reconstructed in different β-values and frame durations	PET-CT imaging data Medical records	PET-CT imaging data Medical records	PET-CT imaging, blood and urine sampling
Statistical analyses	Friedman ranking test, Wilcoxon signed-rank test, Kruskal-Wallis test, Mann-Whitney U-test, Bonferroni corrections for multiple tests	Sensitivity, specificity, the positive predictive value, the negative predictive value	Chi-square test, Mann-Whitney U-test, Sensitivity, specificity, positive predictive value, negative prdeictive value, ROC analyses	

Data and assessment tools

Image analysis (study I)

Quantitatively, the [^{18}F]FCH PET-CT images were analysed regarding SUV in suspected lymph node metastasis, local background, and muscle background to be able to calculate the CNR and the image's noise level as the coefficient of variation.

Assessment and interpretation of images (study I)

Subjective assessments of image quality were made by five nuclear medicine physicians. Interpretations of the number of suspected metastases in lymph nodes in images were made by two experienced nuclear medicine physicians.

Absence/presence of suspected lymph node metastases, [^{18}F]FCH PET-CT vs ePLND (study II and III)

The absence/presence of suspected lymph node metastases detected by the [^{18}F]FCH PET-CT examination was compared with the actual presence of lesions at ePLND to understand the accuracy of the PET-CT technology and radiopharmaceutical in the first diagnostic accuracy study. To understand these results more in-depth, a comparison between the conventional PM-based and the novel SiPM-based PET-CT system in the ability to detect suspected lymph node metastases was performed in a second diagnostic accuracy study. Also, the diagnostic accuracy for metastatic lymph node detections for both PET-CT systems was analysed using an area-under-the-curve receive operating characteristic (ROC) analysis. The studies were made based on the patient's medical records and the clinical report for the PET-CT examination. The clinical report for the pathology was used as reference method in both studies.

Biokinetics and radiation dosimetry (study IV)

The biokinetics of [^{18}F]PSMA-1007 was followed by the region of interests drawn around the organs in the PET-CT images, using the Research Consortium for Medical Image Analysis (RECOMIA) platform (www.recomia.org) (88). Through RECOMIA the amount of activity in the organs for each scan was obtained. Based on the activities in the organs together with the amount of activity in blood and urine, a compartment model was constructed using MATLAB (MathWorks, Natick, MA, USA). From the compartment model, was TACs for each organ produced which was used to calculate the radiation dosimetry of [^{18}F]PSMA-1007 by using

the dosimetry program IDAC-Dose 2.1 (89). From the TACs, IDAC calculated the absorbed dose for each organ and the effective dose for the whole body.

Data management and statistical analyses

All data were entered into IBM SPSS Statistics version 26 (IBM Corp., Armonk, NY, USA) for analysis. Stata 16.0 (StataCorp LLC, College Station, TX, USA) was used to calculate the p-value of the ROC-analysis in the second diagnostic accuracy study.

The data were presented using descriptive and analytic statistics. Non-parametric statistics were used because the data were skewed. For the comparison of contrast-to-noise ratio for the different reconstructions in the optimization study, the Friedman ranking test was used since the same observations was included in all groups. The Wilcoxon signed-rank test was used as a post-hoc test. Differences in image quality between the different reconstructions was examined with the Kruskal-Wallis test. The Mann-Whitney U-test was used for post-hoc comparisons. When testing multiple comparisons, Bonferroni corrections for multiple tests were used.

The diagnostic accuracy of [^{18}F]FCH PET-CT for detecting regional metastases in prostate cancer was examined in the study II and III using histopathology in lymph node dissection as the reference method. Sensitivity, specificity, and positive- and negative predictive values were presented for all patients and analysed based on risk groups in the first diagnostic accuracy study. In study III, sensitivity, specificity, and positive-, and negative predictive values were calculated per patient and per side (right and left). The ROC analyses were used to evaluate the diagnostic test. The comparison of baseline variables for patients examined on either of the different PET-CT systems was made using the Mann-Whitney U-test. A chi-square test was performed to summarize the relationship between group and outcome in the cross tables.

The confidence intervals were 95% for the respective groups in the diagnostic accuracy studies. P-values less than 0.05 were considered statistically significant in all papers.

Ethics

All studies in this thesis comply with the Declaration of Helsinki. The optimization study was regarded as a clinical development assessment with anonymized images before analysis. Therefore, no ethical board evaluation was required according to Swedish law. The other studies were approved by the Regional Ethics Committee in Lund (#2018/690, #2016/417, 2018/750 and #2020-00689, respectively). The participants in all studies gave their written consent before enrolment.

Results

The main findings of the different papers are summarized in this section.

Image analysis (study I)

After injection of 4 MBq/kg [^{18}F]FCH, BSREM with a frame duration of 2.0 min with β 300 showed the highest median CNR (Figure 8). With the increasing value of β, both the lesion SUV_{max} and the noise level decrease. The highest and lowest median lesion SUV_{max} is presented in Figure 9, and the image noise level for the different reconstruction combinations is shown in Figure 10.

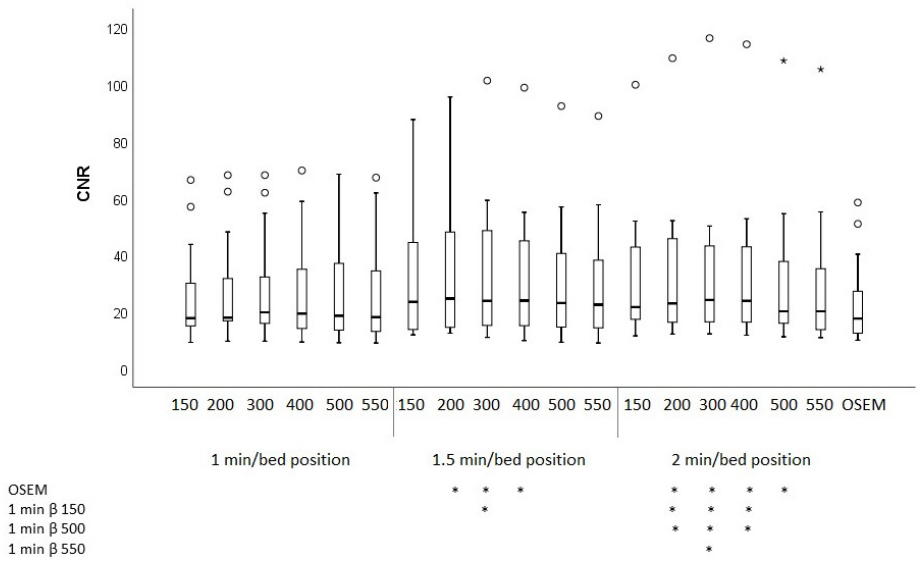

Figure 8. CNR boxplot.
The thick horizontal line represents the median and the box in the interquartile range (IQR). Whiskers represent the non-outlier range. Outliers (1.5 * IQR) and extremes (3 * IQR) are shown by asterisks and circles, respectively. The combinations of reconstruction parameters that reached statistical significance are indicated with stars below the graph.

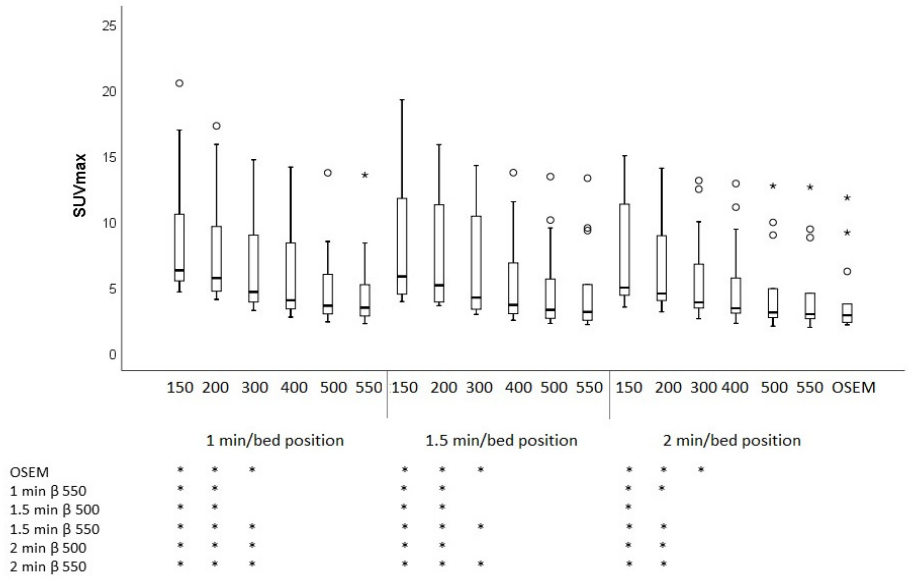

Figure 9. Boxplot of lesion SUV_{max}.
The thick horizontal line represents the median and the box in the interquartile range (IQR). Whiskers represent the non-outlier range. Outliers (1.5 * IQR) and extremes (3 * IQR) are shown by asterisks and circles, respectively. The combinations of reconstruction parameters that reached statistical significance are indicated with stars below the graph.

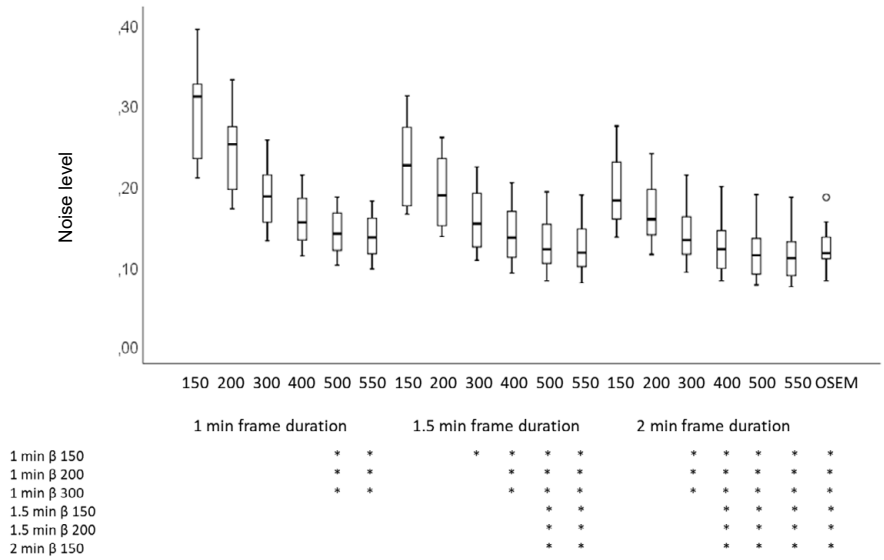

Figure 10. Boxplot of noise level in muscle.
Noise level is calculated as the coefficient of variation. The thick horizontal line represents the median and the box in the interquartile range (IQR). Whiskers represent the non-outlier range. Outliers (1.5 * IQR) and extremes (3 * IQR) are shown by asterisks and circles, respectively. The combinations of reconstruction parameters that reached statistical significance are indicated with stars below the graph. The combinations of reconstruction parameters that reached statistical significance are indicated with stars below the graph.

Assessment and interpretation of images (study I)

The highest median quality score was found for a frame duration of 1.5 min and β 400–500, and for a frame duration of 2.0 min with β 300–500 (Table 5).

The only statistically significant difference within the interpretation of lymph nodes in images was between 1.5 min with β 500 and 2.0 min with β 300 ($p = 0.040$) for one physician.

Table 5. Assessment of image quality
Five physicians assessed the image quality for ten patients on a scale of 1–5 (1 = unacceptable image quality and 5 = very high image quality). The median (and range) and overall image quality score are presented.

	Observers (median, range)					
	#1	#2	#3	#4	#5	Overall
1.5 min, β 300	2 (1–3)	2 (2–4)	2 (1–3)	3 (2–4)	2 (1–2)	2
1.5 min, β 400	3 (1–3)	3 (2–4)	2.5 (2–5)	3 (2–4)	2 (2–3)	3
1.5 min, β 500	3 (3–4)	3 (3–4)	3 (3–4)	3 (2–4)	3 (2–4)	3
2.0 min, β 300	2 (1–3)	3.5 (2–4)	2 (1–5)	4 (3–4)	2 (2–3)	3
2.0 min, β 400	3.5 (1–4)	3 (2–4)	3 (2–4)	3 (2–4)	3 (2–4)	3
2.0 min, β 500	3 (3–4)	3 (2–4)	3 (3–4)	2.5 (2–3)	3.5 (2–4)	3
2.0 min, OSEM	3.5 (2–4)	3 (2–4)	2.5 (1–3)	2 (2)	2.5 (2–3)	2.5

Absence/presence of suspected lymph node metastases, [^{18}F]FCH PET-CT vs ePLND (study II and III)

In the first diagnostic accuracy study, suspected lymph node metastases were found on [^{18}F]FCH PET-CT examinations in 85 (34%) of the 252 included patients. But based on ePLND surgery, only 31 (12%) patients had proven lymph node metastases, which give 54 (21%) patients with false positive [^{18}F]FCH PET-CT examination (Table 6). Sensitivity, specificity, positive predictive value, and negative predictive value for [^{18}F]FCH PET-CT to predict metastatic lymph nodes are presented in Table 7.

Table 6. Detecting suspected lymph node metastases by histopathology and [^{18}F]FCH PET-CT.

		Lymph node status by histopathology		
		Positive	Negative	Total
Lymph node status by PET-CT	Positive	31	54	85
	Negative	41	126	167
	Total	72	180	252

Table 7. Accuracy of [^{18}F]FCH PET-CT.
Sensitivity, specificity, positive predictive value (PPV), and negative predictive value (NPV) for prediction of lymph node metastases by [^{18}F]FCH PET-CT (95% confidence interval) with histopathology report as the reference method.

Accuracy of PET-CT	
Sensitivity	0.43 (0.32–0.55)
Specificity	0.71 (0.63–0.76)
PPV	0.37 (0.27–0.43)
NPV	0.76 (0.68–0.82)

For the second diagnostic accuracy study, 19 (20%) patients examined on the PM-based PET-CT system were regarded as having suspected metastatic lymph nodes, whereas nine (9%) patients were proven to have positive lymph nodes based on histopathology. Thirty-eight (40%) patients examined on the SiPM-based PET-CT system were regarded as having suspected metastatic lymph nodes, whereas 11 (12%) patients were proven to have positive lymph nodes based on histopathology (Table 8).

Sensitivity, specificity, positive predictive value, and negative predictive value per patient and per side for the PM-based and the SiPM-based PET-CT system are presented in Table 9.

The areas under the ROC for the systems were similar: 0.57 for the PM-based PET-CT and 0.58 for the SiPM-based PET-CT ($p = 0.89$).

Table 8. Per patient analysis and per side analysis in detecting lymph node metastases using [^{18}F]FCH the conventional PM-based or the novel SiPM-based PET-CT system.

		Lymph nodes at histopathology		
Lymph nodes at PET-CT		Positive	Negative	Total
Per patient analysis PM-based PET-CT	Positive	9	10	19
	Negative	21	53	74
	Total	30	63	93
SiPM-based PET-CT	Positive	11	27	38
	Negative	8	38	46
	Total	19	65	94
Per side analysis PM-based PET-CT	Positive	6	5	11
	Negative	24	58	82
	Total	30	63	91
SiPM-based PET-CT	Positive	9	21	30
	Negative	10	44	54
	Total	19	65	84

Table 9. Per patient and per side accuracy analysis using different PET-CT systems with [^{18}F]FCH.
Sensitivity, specificity, positive predictive value (PPV), and negative predictive value (NPV) for prediction of lymph node metastases by [^{18}F]FCH PM-based or SiPM-based PET-CT (95% confidence interval) with histopathology report as the reference method.

	Per patient analysis		Per side analysis	
	PM-based PET-CT	SiPM-based PET-CT	PM-based PET-CT	SiPM-based PET-CT
Sensitivity	0.30 (0.17–0.48)	0.58 (0.36–0.77)	0.20 (0.10–0.37)	0.47 (0.27–0.68)
Specificity	0.84 (0.73–0.91)	0.59 (0.46–0.70)	0.92 (0.83–0.97)	0.68 (0.56–0.78)
PPV	0.47 (0.27–0.68)	0.29 (0.17–0.45)	0.55 (0.28–0.79)	0.30 (0.17–0.48)
NPV	0.72 (0.60–0.81)	0.83 (0.69–0.90)	0.71 (0.60–0.80)	0.82 (0.69–0.90)

Biokinetics (study IV)

The activity concentration was high in lacrimal glands, salivary glands, spleen, kidneys, liver, and parts of the small intestine. The concentration increases over time for all these organs, and at the final imaging session at 5.5 h, the decay corrected TACs reached or approached a plateau (Figure 11).

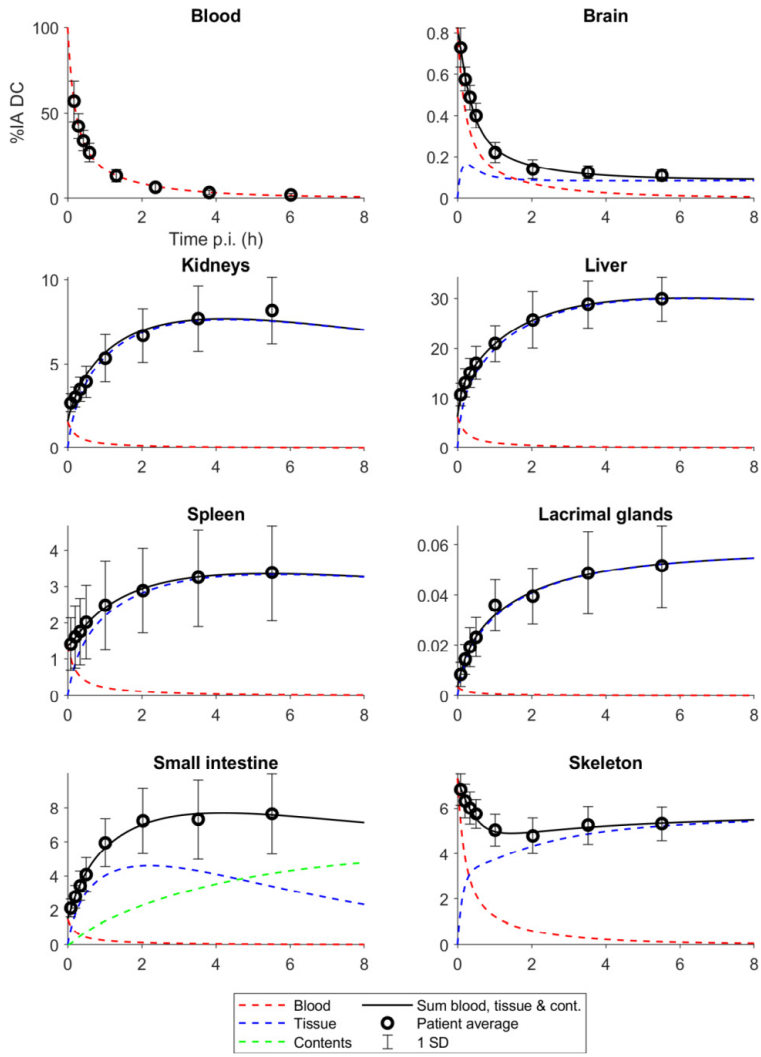

Figure 11. Time-activity curves for [^{18}F]PSMA-1007 in patients with prostate cancer.
Decay corrected time-activity curves (TAC) showing the precentage of injected activity at a certain time. The TACs are developed through the compartments modell.

Radiation dosimetry (study IV)

As shown in Table 10, the highest absorbed dose is obtained in the lacrimal glands, kidneys, salivary glands, liver, and spleen. The effective dose for [^{18}F]PSMA-1007 was 25 µSv/MBq. This means that patients with a 60–100 kg weight who are injected with 4 MBq/kg receive a radiation burden of 6–10 mSv. This radiation burden is of the same order of magnitude as other common radiopharmaceuticals used in oncology, so it supports the continued use of [^{18}F]PSMA-1007.

Tabel 10. Absorbed and effective dose for [18F]PSMA-1007 per injected activity.
Absorbed dosess are in µGy/MBq, and the effective dose is in µSv/MBq.

Organ	Absorbed dose
Adrenals	37.7
Brain	3.40
Breast	10.6
Gallbladder wall	44.7
Heart wall	25.6
Kidneys	84.5
Lacrimal glands	97.6
Left colon	20.6
Liver	70.4
Lungs	23.3
Muscle	7.44
Pancreas	38.0
Prostate	9.09
Recto-sigmoid colon	17.1
Red marrow	21.6
Right colon	26.9
Salivary glands	82.9
Skin	6.50
Small intestine	31.8
Spleen	66.2
Stomach	29.1
Testes	9.42
Thymus	10.0
Thyroid	11.0
Urinary bladder wall	11.6
Effective Dose (ICRP 60)	22.0
Effective Dose (ICRP 103)	24.9

Discussion

This thesis presents various aspects of PET-CT in prostate cancer through real-world observational studies. The aspects were an optimization study that explained which reconstruction parameters contributed to the highest image quality at a given amount of [^{18}F]FCH. Further, a validation study of the diagnostic accuracy of the [^{18}F]FCH PET-CT examination method was compared with a reference method. To understand this result more in-depth, the diagnostic accuracy of the different PET-CT systems was compared in a second study. As the [^{18}F]FCH is not specific or sensitive enough for prostate cancer, this radiopharmaceutical was phased out and replaced by [^{18}F]PSMA-1007. Through biokinetic- and dosimetry studies, the effective doses of [^{18}F]PSMA-1007 was measured. The results support the continued use of the radiopharmaceutical. The thesis contributes further knowledge about what the routine clinical method [^{18}F]FCH and [^{18}F]PSMA-1007 PET-CT produces and adds to the examination of prostate cancer.

In this thesis is the studies retrospective. To meet the aim of each study, patients who met the inclusion criteria were selected to be included meaning there has been no randomization. This, together with the fact that necessary data may be missing is some of the disadvantages of retrospective studies and way they are considered to have a lower degree of scientific evidence than prospective studies.

The number of patients in each paper was based on the purpose of the studies, the availability of patients and their management, and the number of patients used in previous similar studies. There may be a risk of skewed selection of patients in terms of age, PSA value and stage of the disease, etc. There was no statistically significant difference between the groups in these aspects in the studies on diagnostic accuracy. No power calculation has been made for any of the studies.

The method in this dissertation is based on real-world observational studies even though randomised clinical trials (RCTs) are the “gold standard” to understand the efficacy and safety of the medical intervention. RCTs usually give high treatment and diagnostic results due to strict inclusion and exclusion criteria and how to interpret the diagnostic images to reduce the risk of bias. Real-world observational studies evaluate the effectiveness of a diagnostic method in clinical practice, even though the risk for bias is much higher. However, real-world observational studies have become an important complement to RCTs (90-92). Radiolabelled choline was highly valued when it was introduced to the market, and together with the PET-CT systems used at

that time, it provided sufficient and important information about prostate cancer disease. Measured by today's standards with a new generation of PET-CT systems and better radiopharmaceuticals, radiolabelled choline has largely been removed from clinical practice in the management of prostate cancer. However, it is important to ask whether the same approach is being repeated using radiolabelled PSMA, and similar studies should be carried out also for PSMA in the future.

When introducing new PET-CT systems and radiopharmaceuticals, optimization work should be performed. PET-CT systems differ from each other with respect to hardware and software structure, which requires different settings and reconstruction parameters. Also, different radiopharmaceuticals have different uptake in tissues, which requires understanding about the specific radiopharmaceutical. To use a PET-CT examination method to the full, the various aspects need to be considered and the interpretation criteria adjusted. At the start of the optimization study, study I, [^{18}F]FCH PET-CT was already in question regarding its accuracy for detecting prostate cancer lesions. However, [^{18}F]PSMA-1007 had not yet been approved by the Swedish Medical Products Agency at that time; and is still not approved; but since 2019, we may use it on license. Since examination of prostate cancer with PET-CT was performed to a potential greater extent at our clinic at Skåne University Hospital compared to other clinics in Sweden, the [^{18}F]FCH PET-CT was used in these examinations. When new PET-CT systems installation was completed, the optimization study was performed with [^{18}F]FCH PET-CT. Similar optimization studies have also been conducted for [^{18}F]FDG and [^{18}F]PSMA at the clinic (93, 94).

The first diagnostic accuracy study (study II) shows low diagnostic performance for [^{18}F]FCH PET-CT where [^{18}F]FCH is the main factor in the outcome (53). At the same time, the study showed lower sensitivity and specificity compared to previous studies (95). Possible reasons can be patient selection, PET-CT systems, ePLND procedure, and interpretation criteria of images. The patient group in this study was examined on three different PET-CT systems. To test if additional factors were behind the low performance, two of the PET-CT systems were examined in the second study on diagnostic accuracy, study III.

The optimization and diagnostic accuracy studies are based on clinical patient records: PET-CT images and preparations from ePLND. As the PET-CT images and preparations are clinical and assessed by experienced nuclear medicine physicians and uropathologists, respectively, it must be assumed that the assessment is made correctly. However, the human factor remains, and in the chain from when the patient underwent the PET-CT examination to the interpretation of preparations after ePLND, many people are involved. As the interpretation of images is based on subjective assessment, the interpretation is strongly dependent on the observer. However, it is important to maintain reproducibility of the study as far as possible in order to ensure consistency in assessment between observers and clinics in order to establish reliable diagnostic tools. Previous inter-observer variability for

[^{18}F]FCH PET-CT has been studied (96) with moderate inter-observer variability for local recurrence in the prostate (Fleiss' kappa 0.55) and good for lymph node metastases (Fleiss' kappa 0.89). In the optimization study the reviewers may have recognized the images even though the review was spread over time.

Histopathology was used as the reference method for PET-CT in study II and III where ePLND was performed robot-assisted. In robot-assisted prostatectomy, lymph nodes are removed within a predetermined area. Lymph nodes outside this area are not removed as these are difficult to access with the robot-assisted method. In a similar published study (95) open surgery combined with a sentinel node technique and probe at the prostatectomy was used. This allows the metastatic lymph nodes to be found. The study reported higher specificity than the first diagnostic accuracy study in this thesis. One reason for this may be selection bias in that referring physicians may be more restrictive with which patients are referred to a new examination method. As an examination method is more routinely used in clinical practice, the restriction on who is referred for an examination may decrease. This accuracy may have contributed to patients referred to the study having metastatic lymph nodes.

The interpretation of the images and histological preparation in study II and III have not undergone a second review, but the primary clinically given report was used. In future studies, the images and histopathology preparations should be reviewed to minimize the variance between interpretive nuclear medicine physicians as well as pathologists.

A dosimetric study for [^{18}F]PSMA-1007 has previously been done in three healthy volunteers (58). Since the decay rate for (^{18}F) is well known with a half-life of 110 min, and gives moderate radiation doses, [^{18}F]PSMA-1007 is not considered a danger. Based on today's knowledge that [^{18}F]PSMA-1007 saves lives in the patient group, the benefits of the radiopharmaceutical outweigh any possible risk. However, due to possible future screenings of prostate cancer with [^{18}F]PSMA-1007, biokinetic and dosimetry studies are important to conduct. Studies accomplished in the specific patient group with high-risk prostate cancer generates an understanding of the path of the radiopharmaceutical through the body and what retention looks like. The biokinetic study (study IV) was performed with only men with prostate cancer in the study population, the results will therefore not be generalizable. Furthermore, there is also a risk that patients with prostate cancer have a large uptake of the radiopharmaceutical in the tumour, which reduces the amount of activity to the rest of the body, the so-called "tumour-sink-effect". This study design was used because [^{18}F]PSMA-1007 is only used for this patient group at Skåne University Hospital. If, in the future, [^{18}F]PSMA-1007 PET-CT will be used in populations other than prostate cancer patients, dosimetry studies for these study populations will be needed.

Conclusions

The evaluation of [^{18}F]FCH with the conventional PM-based and the new SiPM-based PET platform, and the investigation of the new radiopharmaceutical [^{18}F]PSMA-1007 for patients with prostate cancer provides knowledge about the benefits of the new PET technology - the reconstruction algorithm, the poor performance of [^{18}F]FCH and that the effective dose of [^{18}F]PSMA-1007 supports the continued use of the radiopharmaceutical in the examination of prostate cancer.

- The reconstruction algorithm BSREM is advantageous over OSEM. Given that the new PET-CT system is used and that 4 MBq/kg [^{18}F]FCH is injected, acceptable image quality is obtained at 1.5 min/bed position with a β of 400–550. When using BSREM a lower β should be used if a high CNR is desired and a higher β if a low noise level is important.
- [^{18}F]FCH reduces the diagnostic accuracy of [^{18}F]FCH PET-CT in predicting lymph node metastasis in intermediate and high-risk prostate cancer.
- There is a marked difference in sensitivity and specificity for the different PET-CT systems using [^{18}F]FCH. Independent of the PET-CT system, the overall diagnostic performance was poor, but similar.
- The effective dose of [^{18}F]PSMA-1007 was calculated to 25 μSv/MBq which means 8.0 mSv for a "standard person" injected with 320 MBq. This is comparable to other PSMA radioligands and other commonly used radiopharmaceuticals like FDG, supporting the continued use of [^{18}F]PSMA-1007 as a diagnostic imaging agent in prostate cancer.

Future perspective

When introducing new clinical methods and substances, positive results are often very much in favour of the new methods and substances. Despite such positive results, it is important to be questioning and to have a humble approach. There are high expectations that [^{18}F]PSMA-1007 will improve the PET-CT method in prostate cancer. However, multiple studies on [^{18}F]PSMA-1007 will need to be done in various set-ups, similar to the studies performed with [^{18}F]FCH. A hierarchical model of efficacy for diagnostic imaging studies have been suggested (97). Level 1 concerns technical quality of the images; Level 2 addresses diagnostic accuracy associated with interpretation of the images; Level 3 focuses on whether the information produces change in the referring physician's diagnostic thinking; Level 4 concerns effect on the patient management plan; Level 5 are efficacy studies measuring effect of the information on patient outcomes; Level 6 analyses societal costs and benefits of a diagnostic imaging technology. Demonstration of efficacy at each lower level in the hierarchy is necessary, but not sufficient to assure efficacy at higher levels. In this thesis, Level 1 and 2 are studied. In the future, also higher levels of diagnostic hierarchy should be performed for PSMA PET-CT. Since [^{18}F]PSMA-1007 is not only specific to prostate cancer, it should be further explored if it can be used in more diseases than prostate cancer (98-100).

Acknowledgments

First and foremost, I would like to thank my main supervisor Elin Trägårdh for inviting me to become a PhD student and part of your team and research. Thank you for believing in me and giving me this opportunity to develop as a researcher, develop in my profession and as a human. Thank you for investing your time in me and sharing your knowledge and experience. You have helped me build a solid foundation to further my curiosity.

Thanks to my supervisor, Jenny Oddstig, for informative discussions and conversations about physics, which is experienced as a mystery for me. You have opened up that knowledge for me and made it very interesting. Thank you for always treating me with warmth and being very patient with my thoughts.

Thanks to my supervisors Sophia Zackrisson and Per Wollmer, who have inspired me with their deep knowledge of their respective subjects and invaluable feedback and comments on my work.

I am very grateful for the help and support David Minarik has given me in terms of physics and mathematics in the optimization and diagnostic accuracy studies.

I want to direct a great thanks to Anders Bjartell for allowing me to participate in a robot-assisted prostatectomy and at patient visits at your clinic at the Department of Urology. Those occasions gave me a deeper knowledge of the challenges and opportunities in the diagnosis and investigations of prostate cancer. Thank you for always treating me interestingly and encouragingly.

Thanks to Nina Karindotter-Borgendahl and Helén Almquist for their great co-authorship in the optimization study. And thanks to Ulrika Bitzén and Nicole McMichael for assessing image quality in the study.

Thanks to Christopher Puterman for close collaboration and good co-authorship in the diagnostic accuracy studies. A continued thanks to the other co-authors; Jennifer Amidi, who kept track of all participating patients; Assem Anand, Wolfgang Soller, and Thomas Jiborn, who shared their deep knowledge and good feedback; and Henrik Kjölhede, who shared his experiences of performing similar studies, his knowledge and feedback.

Thank you, Erland Hvittfeldt, for your collaboration and co-authorship in the biokinetic study. Thank you for sharing old and new knowledge with me. A continued thanks to all the other co-authors, Gustav Brolin and Sigrid Leide Svergborn who explained the physics and shared their deep knowledge with me.

And thanks to the PET Research in Skåne (PETRiS) research group for allowing me to be a part of the community and participate in everyone's research. Thank you for the support and feedback during the exercise before the half-time review and the test dissertation. Good luck with your continued research.

I would like to also thank Anna Åkesson, a statistician at Region Skåne, for statistical advice. I have learned a lot through our mail conversations.

I am so happy and very thankful for reaching new friends through my PhD-studies. Being able to share the different challenges of education and share thoughts with someone in the same situation I have experienced as having made it easier. Getting to know you, Linn Rosell, during the compulsory doctoral courses was a great joy for me. To share pieces of our lives with all that it means during our lunches, I have always looked forward to and appreciated. And Anni Gålne, to have the opportunity to get to know you and for a period, to share some of the greatest in life during our pregnancies – it is doing something with a relationship with a new friend. I am grateful we had time to hang out a bit before the pandemic.

Thank you Barbro Kjellström, Mariam Al-Mashat, Andreas Malmgren and Abir Nasr for inspiring, informative, and fun meetings together. Being able to discuss texts, situations, and thoughts together with you has contributed to my development and having fun along the way.

My work would not have been possible to perform if it were not for all my colleagues at the Department of Clinical Physiology and Nuclear Medicine, Skåne University Hospital. Thank you for collecting data, thank you for allowing me to practice my presentations on you and thank you for allowing me to be one of the gang even when I have not worked clinically.

Ann-Marie and Richard, Henric, Linda and Eric with families, thank you for welcoming me into your family and making worries about work seem very distant.

Mom and Dad, I am moved to tears of love and gratitude for you. I know you are very proud of me; at the same time, I know that I do not have to do anything to make you prouder than just being myself. And even though I will soon be a "doctor", it still feels like I am your little girl who sometimes needs to get up in your arms and just be small.

Olivia and William, the boundless love I feel for you is indescribable. You make me very proud. And thank you for choosing such wonderful persons to share your life with. Tobias and Anna, to have received you into my family is a gift.

And Patric, my love and rock in life. I cannot describe in words how much I love you because tears of gratitude already flow when I think of us. Thank you, my sweetheart!

And Selma and Lovisa, my girls, remember that Mom loves you just for who you are and that nothing can make that love greater or less. I am so grateful for you, and it is a privilege to follow you through your lives.

References

1. N. Mottet (Chair) PCV-c, R.C.N. van den Bergh, E. Briers, Expert Patient Advocate (European Prostate Cancer Coalition/Europa UOMO), M. De Santis, S. Gillessen, J. Grummet, A.M. Henry, T.H. van der Kwast, T.B. Lam, M.D. Mason, S. O'Hanlon, D.E. Oprea-Lager, G. Ploussard, H.G. van der Poel, O. Rouvière, I.G. Schoots, D. Tilki, T. Wiegel, Guidelines Associates: T. Van den Broeck MC, A. Farolfi, N. Fossati, G. Gandaglia, N. Grivas, M. Lardas, M. Liew, L. Moris, P-P.M. Willemse. EAU-EANM-ESTRO-ESUR-ISUP-SIOG-Guidelines on Prostate Cancer [Internet]. The Netherlands; 2021 [cited 2022 January 5]. Available from: https://uroweb.org/guideline/prostate-cancer/.
2. Regionala cancercentrum i samverkan. Nationellt vårdprogram för prostatacancer [National Prostate Cancer Care Program] [Internet]. Stockholm; 2021 [cited 2022 January 5]. Available from: https://kunskapsbanken.cancercentrum.se/diagnoser/prostatacancer/vardprogram/.
3. Bailey D, L.; Townsend, D, W.; Valk, P, E.; Maisey, M, N. Positron Emission Tomography London: Springer; 2005 [cited 2021 12-14].
4. Cherry SR. Physics in Nuclear Medicine. Philadelphia, PA, USA: W B Saunders Company; 2012.
5. Oddstig J, Leide Svegborn S, Almquist H, Bitzén U, Garpered S, Hedeer F, et al. Comparison of conventional and Si-photomultiplier-based PET systems for image quality and diagnostic performance. BMC medical imaging. 2019;19(1):81.
6. van der Vos CS, Koopman D, Rijnsdorp S, Arends AJ, Boellaard R, van Dalen JA, et al. Quantification, improvement, and harmonization of small lesion detection with state-of-the-art PET. Eur J Nucl Med Mol Imaging. 2017;44(Suppl 1):4-16.
7. Bouchelouche K, Turkbey B, Choyke PL. PSMA PET and Radionuclide Therapy in Prostate Cancer. Semin Nucl Med. 2016;46(6):522-35.
8. Socialstyrelsen. Statistik om nyupptäckta cancerfall 20192020 [cited 2021 04-29]. Available from: https://www.socialstyrelsen.se/globalassets/sharepoint-dokument/artikelkatalog/statistik/2020-12-7132.pdf.
9. Jones T, Townsend D. History and future technical innovation in positron emission tomography. J Med Imaging (Bellingham). 2017;4(1):011013.
10. Zhou J, Gou Z, Wu R, Yuan Y, Yu G, Zhao Y. Comparison of PSMA-PET/CT, choline-PET/CT, NaF-PET/CT, MRI, and bone scintigraphy in the diagnosis of bone metastases in patients with prostate cancer: a systematic review and meta-analysis. Skeletal Radiol. 2019;48(12):1915-24.
11. Powers GL, Marker PC. Recent advances in prostate development and links to prostatic diseases. Wiley Interdiscip Rev Syst Biol Med. 2013;5(2):243-56.

12. Elaine N M, Katja H. Human anatomy & physiology. Global edition; Eighth edition ed: San Francisco : Pearson Benjamin Cummings, cop 2010; 2010.
13. Ittmann M. Anatomy and Histology of the Human and Murine Prostate. Cold Spring Harb Perspect Med. 2018;8(5).
14. Aaron L, Franco OE, Hayward SW. Review of Prostate Anatomy and Embryology and the Etiology of Benign Prostatic Hyperplasia. Urol Clin North Am. 2016;43(3):279-88.
15. McNeal JE. Anatomy of the prostate and morphogenesis of BPH. Prog Clin Biol Res. 1984;145:27-53.
16. Klein EA, Thompson IM, Jr., Tangen CM, Crowley JJ, Lucia MS, Goodman PJ, et al. Vitamin E and the risk of prostate cancer: the Selenium and Vitamin E Cancer Prevention Trial (SELECT). Jama. 2011;306(14):1549-56.
17. Lippman SM, Klein EA, Goodman PJ, Lucia MS, Thompson IM, Ford LG, et al. Effect of selenium and vitamin E on risk of prostate cancer and other cancers: the Selenium and Vitamin E Cancer Prevention Trial (SELECT). Jama. 2009;301(1):39-51.
18. Socialstyrelsen. Screening för prostatacancer2018 [cited 2021 04-29]. Available from: https://www.socialstyrelsen.se/globalassets/sharepoint-dokument/artikelkatalog/nationella-screeningprogram/2018-10-15.pdf.
19. Eklund M, Jäderling F, Discacciati A, Bergman M, Annerstedt M, Aly M, et al. MRI-Targeted or Standard Biopsy in Prostate Cancer Screening. N Engl J Med. 2021;385(10):908-20.
20. Nordström T, Discacciati A, Bergman M, Clements M, Aly M, Annerstedt M, et al. Prostate cancer screening using a combination of risk-prediction, MRI, and targeted prostate biopsies (STHLM3-MRI): a prospective, population-based, randomised, open-label, non-inferiority trial. Lancet Oncol. 2021;22(9):1240-9.
21. Grönberg H, Eklund M, Picker W, Aly M, Jäderling F, Adolfsson J, et al. Prostate Cancer Diagnostics Using a Combination of the Stockholm3 Blood Test and Multiparametric Magnetic Resonance Imaging. Eur Urol. 2018;74(6):722-8.
22. Gandaglia G, Abdollah F, Schiffmann J, Trudeau V, Shariat SF, Kim SP, et al. Distribution of metastatic sites in patients with prostate cancer: A population-based analysis. Prostate. 2014;74(2):210-6.
23. Lilja H. Structure and function of prostatic- and seminal vesicle-secreted proteins involved in the gelation and liquefaction of human semen. Scand J Clin Lab Invest Suppl. 1988;191:13-20.
24. Ito K, Yamamoto T, Ohi M, Kurokawa K, Suzuki K, Yamanaka H. Free/total PSA ratio is a powerful predictor of future prostate cancer morbidity in men with initial PSA levels of 4.1 to 10.0 ng/mL. Urology. 2003;61(4):760-4.
25. Epstein JI, Allsbrook WC, Jr., Amin MB, Egevad LL. The 2005 International Society of Urological Pathology (ISUP) Consensus Conference on Gleason Grading of Prostatic Carcinoma. Am J Surg Pathol. 2005;29(9):1228-42.
26. Gleason DF. Classification of prostatic carcinomas. Cancer Chemother Rep. 1966;50(3):125-8.

27. Epstein JI, Egevad L, Amin MB, Delahunt B, Srigley JR, Humphrey PA. The 2014 International Society of Urological Pathology (ISUP) Consensus Conference on Gleason Grading of Prostatic Carcinoma: Definition of Grading Patterns and Proposal for a New Grading System. Am J Surg Pathol. 2016;40(2):244-52.
28. Egevad L, Delahunt B, Srigley JR, Samaratunga H. International Society of Urological Pathology (ISUP) grading of prostate cancer - An ISUP consensus on contemporary grading. Apmis. 2016;124(6):433-5.
29. Cheung DC, Fleshner N, Sengupta S, Woon D. A narrative review of pelvic lymph node dissection in prostate cancer. Transl Androl Urol. 2020;9(6):3049-55.
30. Stranne J, Brasso K, Brennhovd B, Johansson E, Jäderling F, Kouri M, et al. SPCG-15: a prospective randomized study comparing primary radical prostatectomy and primary radiotherapy plus androgen deprivation therapy for locally advanced prostate cancer. Scand J Urol. 2018;52(5-6):313-20.
31. Moris L, Cumberbatch MG, Van den Broeck T, Gandaglia G, Fossati N, Kelly B, et al. Benefits and Risks of Primary Treatments for High-risk Localized and Locally Advanced Prostate Cancer: An International Multidisciplinary Systematic Review. Eur Urol. 2020;77(5):614-27.
32. D'Amico AV, Whittington R, Malkowicz SB, Schultz D, Blank K, Broderick GA, et al. Biochemical outcome after radical prostatectomy, external beam radiation therapy, or interstitial radiation therapy for clinically localized prostate cancer. Jama. 1998;280(11):969-74.
33. D'Amico AV, Whittington R, Malkowicz SB, Cote K, Loffredo M, Schultz D, et al. Biochemical outcome after radical prostatectomy or external beam radiation therapy for patients with clinically localized prostate carcinoma in the prostate specific antigen era. Cancer. 2002;95(2):281-6.
34. Roach M, 3rd, Hanks G, Thames H, Jr., Schellhammer P, Shipley WU, Sokol GH, et al. Defining biochemical failure following radiotherapy with or without hormonal therapy in men with clinically localized prostate cancer: recommendations of the RTOG-ASTRO Phoenix Consensus Conference. Int J Radiat Oncol Biol Phys. 2006;65(4):965-74.
35. Bouchelouche K, Tagawa ST, Goldsmith SJ, Turkbey B, Capala J, Choyke P. PET/CT Imaging and Radioimmunotherapy of Prostate Cancer. Semin Nucl Med. 2011;41(1):29-44.
36. Treglia G. Diagnostic Performance of (18)F-FDG PET/CT in Infectious and Inflammatory Diseases according to Published Meta-Analyses. Contrast Media Mol Imaging. 2019;2019:3018349.
37. Gaemperli O, Kaufmann PA. PET and PET/CT in cardiovascular disease. Ann N Y Acad Sci. 2011;1228:109-36.
38. Gallamini A, Zwarthoed C, Borra A. Positron Emission Tomography (PET) in Oncology. Cancers (Basel). 2014;6(4):1821-89.
39. Janelidze S, Stomrud E, Smith R, Palmqvist S, Mattsson N, Airey DC, et al. Cerebrospinal fluid p-tau217 performs better than p-tau181 as a biomarker of Alzheimer's disease. Nat Commun. 2020;11(1):1683.

40. Evidence-based Positron Emission Tomography. Cham, Switzerland: Springer Nature Switzerland AG; 2020.
41. Jadvar H. Prostate cancer: PET with 18F-FDG, 18F- or 11C-acetate, and 18F- or 11C-choline. J Nucl Med. 2011;52(1):81-9.
42. Jadvar H. Is There Use for FDG-PET in Prostate Cancer? Semin Nucl Med. 2016;46(6):502-6.
43. Boellaard R, Delgado-Bolton R, Oyen WJ, Giammarile F, Tatsch K, Eschner W, et al. FDG PET/CT: EANM procedure guidelines for tumour imaging: version 2.0. Eur J Nucl Med Mol Imaging. 2015;42(2):328-54.
44. Chernyak V. Novel imaging modalities for lymph node imaging in urologic oncology. Urol Clin North Am. 2011;38(4):471-81, vii.
45. Dave A, Hansen N, Downey R, Johnson C. FDG-PET Imaging of Dementia and Neurodegenerative Disease. Semin Ultrasound CT MR. 2020;41(6):562-71.
46. Ghafoor S, Burger IA, Vargas AH. Multimodality Imaging of Prostate Cancer. J Nucl Med. 2019;60(10):1350-8.
47. Regula N, Häggman M, Johansson S, Sörensen J. Malignant lipogenesis defined by (11)C-acetate PET/CT predicts prostate cancer-specific survival in patients with biochemical relapse after prostatectomy. Eur J Nucl Med Mol Imaging. 2016;43(12):2131-8.
48. Oyama N, Miller TR, Dehdashti F, Siegel BA, Fischer KC, Michalski JM, et al. 11C-acetate PET imaging of prostate cancer: detection of recurrent disease at PSA relapse. J Nucl Med. 2003;44(4):549-55.
49. Buchegger F, Garibotto V, Zilli T, Allainmat L, Jorcano S, Vees H, et al. First imaging results of an intraindividual comparison of (11)C-acetate and (18)F-fluorocholine PET/CT in patients with prostate cancer at early biochemical first or second relapse after prostatectomy or radiotherapy. Eur J Nucl Med Mol Imaging. 2014;41(1):68-78.
50. Regula N, Kostaras V, Johansson S, Trampal C, Lindström E, Lubberink M, et al. Comparison of (68)Ga-PSMA-11 PET/CT with (11)C-acetate PET/CT in re-staging of prostate cancer relapse. Sci Rep. 2020;10(1):4993.
51. Beheshti M, Rezaee A, Geinitz H, Loidl W, Pirich C, Langsteger W. Evaluation of Prostate Cancer Bone Metastases with 18F-NaF and 18F-Fluorocholine PET/CT. J Nucl Med. 2016;57(Suppl 3):55s-60s.
52. Giussani A, Janzen T, Uusijärvi-Lizana H, Tavola F, Zankl M, Sydoff M, et al. A compartmental model for biokinetics and dosimetry of 18F-choline in prostate cancer patients. J Nucl Med. 2012;53(6):985-93.
53. Puterman C, Björsdorff M, Amidi J, Anand A, Soller W, Jiborn T, et al. A retrospective study assessing the accuracy of [18F]-fluorocholine PET/CT for primary staging of lymph node metastases in intermediate and high-risk prostate cancer patients undergoing robotic-assisted laparoscopic prostatectomy with extended lymph node dissection. Scand J Urol. 2021;55(4):293-7.
54. Bjoersdorff MP, C.; Oddstig, J.; Amidi, J.; Zackrisson, S.; Kjolhede, H.; Bjartell, A.; Wollmer, P.; Tragardh, E. Detection of lymph node metastases in patients with prostate cancer: comparing conventional and digital [18F]fluorocholine PET-CT using histopathology as reference. 2021.

55. Anttinen M, Ettala O, Malaspina S, Jambor I, Sandell M, Kajander S, et al. A Prospective Comparison of (18)F-prostate-specific Membrane Antigen-1007 Positron Emission Tomography Computed Tomography, Whole-body 1.5 T Magnetic Resonance Imaging with Diffusion-weighted Imaging, and Single-photon Emission Computed Tomography/Computed Tomography with Traditional Imaging in Primary Distant Metastasis Staging of Prostate Cancer (PROSTAGE). Eur Urol Oncol. 2020.
56. Sprute K, Kramer V, Koerber SA, Meneses M, Fernandez R, Soza-Ried C, et al. Diagnostic Accuracy of (18)F-PSMA-1007 PET/CT Imaging for Lymph Node Staging of Prostate Carcinoma in Primary and Biochemical Recurrence. J Nucl Med. 2021;62(2):208-13.
57. Rauscher I, Krönke M, König M, Gafita A, Maurer T, Horn T, et al. Matched-Pair Comparison of (68)Ga-PSMA-11 PET/CT and (18)F-PSMA-1007 PET/CT: Frequency of Pitfalls and Detection Efficacy in Biochemical Recurrence After Radical Prostatectomy. J Nucl Med. 2020;61(1):51-7.
58. Giesel FL, Hadaschik B, Cardinale J, Radtke J, Vinsensia M, Lehnert W, et al. F-18 labelled PSMA-1007: biodistribution, radiation dosimetry and histopathological validation of tumor lesions in prostate cancer patients. Eur J Nucl Med Mol Imaging. 2017;44(4):678-88.
59. Hsu DFC, Ilan E, Peterson WT, Uribe J, Lubberink M, Levin CS. Studies of a Next-Generation Silicon-Photomultiplier-Based Time-of-Flight PET/CT System. J Nucl Med. 2017;58(9):1511-8.
60. Wagatsuma K, Miwa K, Sakata M, Oda K, Ono H, Kameyama M, et al. Comparison between new-generation SiPM-based and conventional PMT-based TOF-PET/CT. Physica medica : PM : an international journal devoted to the applications of physics to medicine and biology : official journal of the Italian Association of Biomedical Physics (AIFB). 2017;42:203-10.
61. Baratto L, Park SY, Hatami N, Davidzon G, Srinivas S, Gambhir SS, et al. 18F-FDG silicon photomultiplier PET/CT: A pilot study comparing semi-quantitative measurements with standard PET/CT. PloS one. 2017;12(6):e0178936.
62. Nguyen NC, Vercher-Conejero JL, Sattar A, Miller MA, Maniawski PJ, Jordan DW, et al. Image Quality and Diagnostic Performance of a Digital PET Prototype in Patients with Oncologic Diseases: Initial Experience and Comparison with Analog PET. J Nucl Med. 2015;56(9):1378-85.
63. Ross S. Q. Clear. GE Healthcare, White Paper. 2014:1-9.
64. Bjöersdorff M, Oddstig J, Karindotter-Borgendahl N, Almquist H, Zackrisson S, Minarik D, et al. Impact of penalizing factor in a block-sequential regularized expectation maximization reconstruction algorithm for (18)F-fluorocholine PET-CT regarding image quality and interpretation. EJNMMI Phys. 2019;6(1):5.
65. Economou Lundeberg J, Oddstig J, Bitzén U, Trägårdh E. Comparison between silicon photomultiplier-based and conventional PET/CT in patients with suspected lung cancer-a pilot study. EJNMMI research. 2019;9(1):35.
66. Lindstrom E, Sundin A, Trampal C, Lindsjo L, Ilan E, Danfors T, et al. Evaluation of penalized likelihood estimation reconstruction on a digital time-of-flight PET/CT scanner for (18)F-FDG whole-body examinations. J Nucl Med. 2018;59(7):1152-8.

67. Teoh EJ, McGowan DR, Macpherson RE, Bradley KM, Gleeson FV. Phantom and Clinical Evaluation of the Bayesian Penalized Likelihood Reconstruction Algorithm Q.Clear on an LYSO PET/CT System. J Nucl Med. 2015;56(9):1447-52.
68. Sah BR, Stolzmann P, Delso G, Wollenweber SD, Hullner M, Hakami YA, et al. Clinical evaluation of a block sequential regularized expectation maximization reconstruction algorithm in 18F-FDG PET/CT studies. Nucl Med Commun. 2017;38(1):57-66.
69. Howard BA, Morgan R, Thorpe MP, Turkington TG, Oldan J, James OG, et al. Comparison of Bayesian penalized likelihood reconstruction versus OS-EM for characterization of small pulmonary nodules in oncologic PET/CT. Ann Nucl Med. 2017;31(8):623-8.
70. Texte E, Gouel P, Thureau S, Lequesne J, Barres B, Edet-Sanson A, et al. Impact of the Bayesian penalized likelihood algorithm (Q.Clear®) in comparison with the OSEM reconstruction on low contrast PET hypoxic images. EJNMMI Phys. 2020;7(1):28.
71. Adams MC, Turkington TG, Wilson JM, Wong TZ. A systematic review of the factors affecting accuracy of SUV measurements. AJR American journal of roentgenology. 2010;195(2):310-20.
72. Montilla-Soler JL, Makanji R. Skeletal Scintigraphy. Cancer Control. 2017;24(2):137-46.
73. Pauwels EK, Stokkel MP. Radiopharmaceuticals for bone lesions. Imaging and therapy in clinical practice. Q J Nucl Med. 2001;45(1):18-26.
74. Schirrmeister H, Guhlmann A, Elsner K, Kotzerke J, Glatting G, Rentschler M, et al. Sensitivity in detecting osseous lesions depends on anatomic localization: planar bone scintigraphy versus 18F PET. J Nucl Med. 1999;40(10):1623-9.
75. Matthias H. CT Teaching Manual: A Systematic Approach to CT Reading. 4th English edition ed: Georg Thieme Verlag KG; 2010.
76. Groves AM, Beadsmoore CJ, Cheow HK, Balan KK, Courtney HM, Kaptoge S, et al. Can 16-detector multislice CT exclude skeletal lesions during tumour staging? Implications for the cancer patient. Eur Radiol. 2006;16(5):1066-73.
77. Wang G, Zhao D, Spring DJ, DePinho RA. Genetics and biology of prostate cancer. Genes Dev. 2018;32(17-18):1105-40.
78. Hofman MS, Lawrentschuk N, Francis RJ, Tang C, Vela I, Thomas P, et al. Prostate-specific membrane antigen PET-CT in patients with high-risk prostate cancer before curative-intent surgery or radiotherapy (proPSMA): a prospective, randomised, multicentre study. Lancet. 2020;395(10231):1208-16.
79. Maurer T, Gschwend JE, Rauscher I, Souvatzoglou M, Haller B, Weirich G, et al. Diagnostic Efficacy of (68)Gallium-PSMA Positron Emission Tomography Compared to Conventional Imaging for Lymph Node Staging of 130 Consecutive Patients with Intermediate to High Risk Prostate Cancer. J Urol. 2016;195(5):1436-43.
80. Carr MW, Grey ML. Magnetic resonance imaging. Am J Nurs. 2002;102(12):26-33.
81. Lecouvet FE, El Mouedden J, Collette L, Coche E, Danse E, Jamar F, et al. Can whole-body magnetic resonance imaging with diffusion-weighted imaging replace Tc 99m bone scanning and computed tomography for single-step detection of metastases in patients with high-risk prostate cancer? Eur Urol. 2012;62(1):68-75.

82. Shen G, Deng H, Hu S, Jia Z. Comparison of choline-PET/CT, MRI, SPECT, and bone scintigraphy in the diagnosis of bone metastases in patients with prostate cancer: a meta-analysis. Skeletal Radiol. 2014;43(11):1503-13.
83. Venkitaraman R, Cook GJ, Dearnaley DP, Parker CC, Huddart RA, Khoo V, et al. Does magnetic resonance imaging of the spine have a role in the staging of prostate cancer? Clin Oncol (R Coll Radiol). 2009;21(1):39-42.
84. Schoots IG, Roobol MJ, Nieboer D, Bangma CH, Steyerberg EW, Hunink MG. Magnetic resonance imaging-targeted biopsy may enhance the diagnostic accuracy of significant prostate cancer detection compared to standard transrectal ultrasound-guided biopsy: a systematic review and meta-analysis. Eur Urol. 2015;68(3):438-50.
85. Drost FH, Osses DF, Nieboer D, Steyerberg EW, Bangma CH, Roobol MJ, et al. Prostate MRI, with or without MRI-targeted biopsy, and systematic biopsy for detecting prostate cancer. Cochrane Database Syst Rev. 2019;4(4):Cd012663.
86. Bolch WE, Eckerman KF, Sgouros G, Thomas SR. MIRD pamphlet No. 21: a generalized schema for radiopharmaceutical dosimetry--standardization of nomenclature. J Nucl Med. 2009;50(3):477-84.
87. Siegel JA, Thomas SR, Stubbs JB, Stabin MG, Hays MT, Koral KF, et al. MIRD pamphlet no. 16: Techniques for quantitative radiopharmaceutical biodistribution data acquisition and analysis for use in human radiation dose estimates. J Nucl Med. 1999;40(2):37s-61s.
88. Trägårdh E, Borrelli P, Kaboteh R, Gillberg T, Ulén J, Enqvist O, et al. RECOMIA-a cloud-based platform for artificial intelligence research in nuclear medicine and radiology. EJNMMI Phys. 2020;7(1):51.
89. Andersson M, Johansson L, Eckerman K, Mattsson S. IDAC-Dose 2.1, an internal dosimetry program for diagnostic nuclear medicine based on the ICRP adult reference voxel phantoms. EJNMMI research. 2017;7(1):88.
90. Tashkin DP, Amin AN, Kerwin EM. Comparing Randomized Controlled Trials and Real-World Studies in Chronic Obstructive Pulmonary Disease Pharmacotherapy. Int J Chron Obstruct Pulmon Dis. 2020;15:1225-43.
91. Monti S, Grosso V, Todoerti M, Caporali R. Randomized controlled trials and real-world data: differences and similarities to untangle literature data. Rheumatology (Oxford). 2018;57(57 Suppl 7):vii54-vii8.
92. Blonde L, Khunti K, Harris SB, Meizinger C, Skolnik NS. Interpretation and Impact of Real-World Clinical Data for the Practicing Clinician. Adv Ther. 2018;35(11):1763-74.
93. Trägårdh E, Minarik D, Almquist H, Bitzén U, Garpered S, Hvittfelt E, et al. Impact of acquisition time and penalizing factor in a block-sequential regularized expectation maximization reconstruction algorithm on a Si-photomultiplier-based PET-CT system for (18)F-FDG. EJNMMI research. 2019;9(1):64.
94. Trägårdh E, Minarik D, Brolin G, Bitzén U, Olsson B, Oddstig J. Optimization of [(18)F]PSMA-1007 PET-CT using regularized reconstruction in patients with prostate cancer. EJNMMI Phys. 2020;7(1):31.
95. Kjolhede H, Ahlgren G, Almquist H, Liedberg F, Lyttkens K, Ohlsson T, et al. (1)(8)F-fluorocholine PET/CT compared with extended pelvic lymph node dissection in high-risk prostate cancer. World journal of urology. 2014;32(4):965-70.

96. Pegard C, Gallazzini-Crépin C, Giai J, Dubreuil J, Caoduro C, Desruet MD, et al. Study of inter- and intra-observer reproducibility in the interpretation of [(18)F]choline PET/CT examinations in patients suffering from biochemically recurrent prostate cancer following curative treatment. EJNMMI research. 2014;4:25.
97. Fryback DG, Thornbury JR. The efficacy of diagnostic imaging. Med Decis Making. 1991;11(2):88-94.
98. Sheikhbahaei S, Afshar-Oromieh A, Eiber M, Solnes LB, Javadi MS, Ross AE, et al. Pearls and pitfalls in clinical interpretation of prostate-specific membrane antigen (PSMA)-targeted PET imaging. Eur J Nucl Med Mol Imaging. 2017;44(12):2117-36.
99. Schmidt LH, Heitkötter B, Schulze AB, Schliemann C, Steinestel K, Trautmann M, et al. Prostate specific membrane antigen (PSMA) expression in non-small cell lung cancer. PloS one. 2017;12(10):e0186280.
100. Dumas F, Gala JL, Berteau P, Brasseur F, Eschwège P, Paradis V, et al. Molecular expression of PSMA mRNA and protein in primary renal tumors. Int J Cancer. 1999;80(6):799-803.